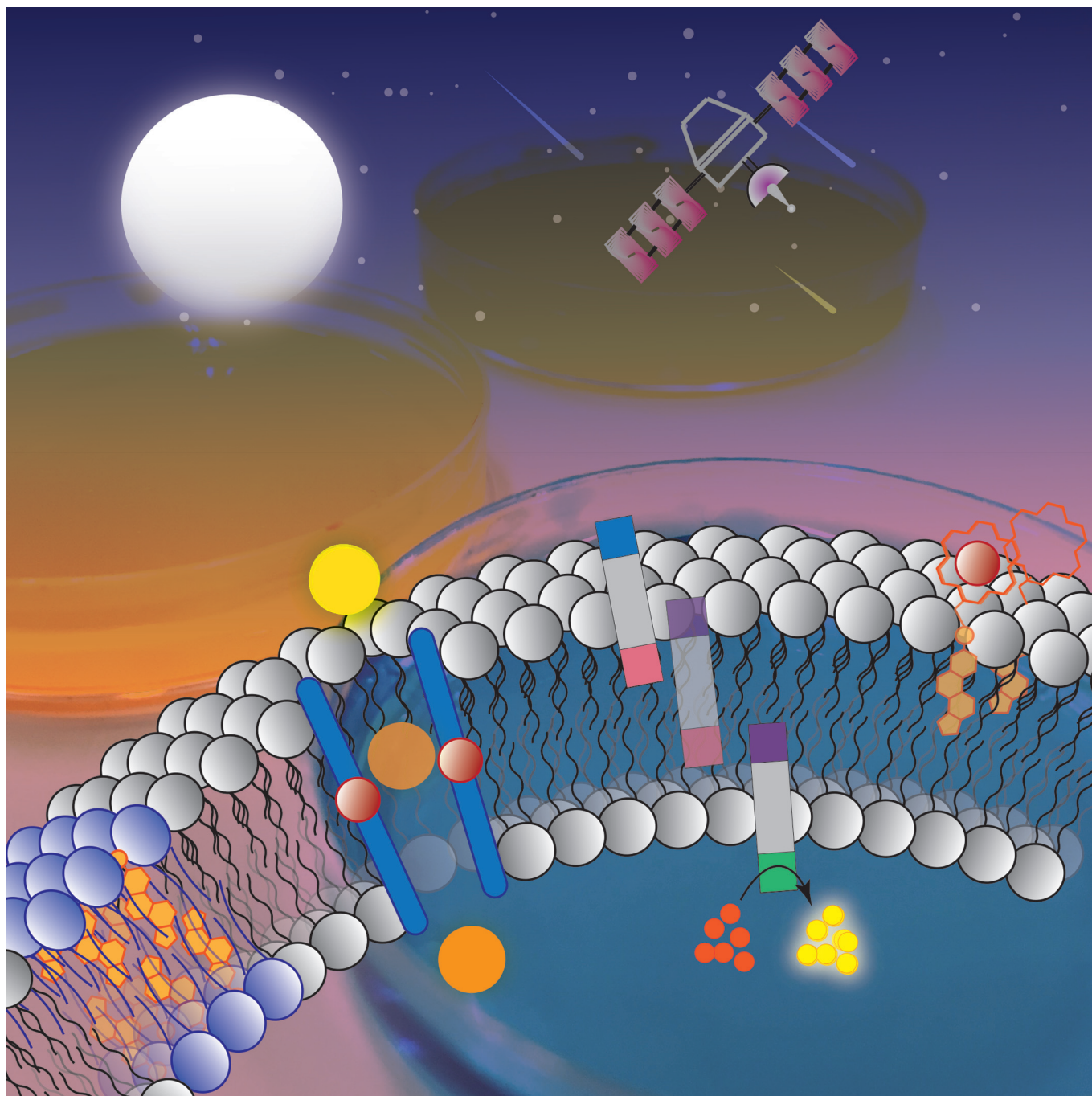


Supramolecular Chemistry in the Biomembrane

Andrea Barba-Bon, Mohamed Nilam, and Andreas Hennig^{*[a]}



The combination of supramolecular functional systems with biomolecular chemistry has been a fruitful exercise for decades, leading to a greater understanding of biomolecules and to a great variety of applications, for example, in drug delivery and sensing. Within these developments, the phospholipid bilayer membrane, surrounding live cells, with all its functions

has also intrigued supramolecular chemists. Herein, recent efforts from the supramolecular chemistry community to mimic natural functions of lipid membranes, such as sensing, molecular recognition, membrane fusion, signal transduction, and gated transport, are reviewed.

1. Introduction

Biomembranes composed of phospholipid molecules are an essential part of all living systems and enable the cell to compartmentalize and separate the intracellular cytosol from its environment. In addition to phospholipids, natural cellular membranes contain a large number of different molecules, for example, membrane proteins, ion channels, and steroids, that exert specific functions. Essentially, the biomembrane was first described as a fluid mosaic.^[1] Extracellular binding to membrane receptors initiates intracellular enzymatic reaction cascades, which enable the cell to sense and respond to environmental changes. Carefully controlled membrane pores and ion channels enable the uptake of nutrients and the excretion of metabolites. Furthermore, some of the most sophisticated functions of living organisms, such as photosynthesis and respiration, are hosted within the biomembrane. Owing to this plethora of different functions, membrane research is at its heart interdisciplinary and ranges from molecular biology to physics. Researchers interested in biomembranes often consider themselves to be biophysical chemists, thereby underlining the highly interdisciplinary nature of this research field.

A similarly highly interdisciplinary research area is supramolecular chemistry, which has received, since its infancy several decades ago, increasing interest from biologists, environmental scientists, engineers, physicists, mathematicians, and others.^[2] The design and study of supramolecular systems involves synthetic compounds not present in nature, but the complexity and functionality of biological systems has always been a major source of inspiration for supramolecular chemists. Examples include the efforts of supramolecular chemists to create artificial enzymes,^[3] the discovery of crown ethers, which can transport cations across hydrophobic barriers similar to natural ionophores, such as valinomycin,^[4] or the design of molecules that fold into predefined, three-dimensional structures reminiscent of folded proteins.^[5]

The definition of the field of supramolecular chemistry has undergone various transitions, since the first mention of the term, and one definition is “the chemistry of the noncovalent bond”.^[2] Weak, noncovalent interactions are thus at the core of supramolecular chemistry, which, accordingly, naturally intersects with ubiquitous noncovalent interactions in biological systems. For example, the driving force for the formation of the lipid bilayer from amphiphilic phospholipids is the hydrophobic effect,^[6] which is an essentially supramolecular interaction of significant current interest.^[7]

Herein, we focus our review on research that designs synthetic models with the goal of mimicking specific functions that are present in natural biomembranes composed of phospholipids. This includes signaling, signal transduction, catalysis, and selected examples from membrane transport. The last topic has advanced rapidly and nowadays is a field in its own right; a comprehensive treatment is thus beyond the scope of this contribution and the reader is referred to excellent regularly updated reviews of this field.^[8]


The systems presented herein work in the natural environment of the phospholipid membrane and their study provides clues and inspiration for the molecular mechanisms of natural systems. Moreover, the presented systems are entirely artificial, but work in natural biomembranes, and thus, pave the way for potential systems that interact bio-orthogonally with living cells in the future. This may lead to new therapeutics and new separation, purification, and sensing technologies. We start with a brief introduction to biomembranes to provide the relevant background material for researchers who are not entirely familiar with the properties of the biomembrane. In subsequent sections, we then introduce selected examples to illustrate the current state of the art in combining supramolecular chemistry with biomembranes.


2. Structure and Properties of Biomembranes

2.1. Phospholipids and the lipid bilayer

Biomembranes are bilayers of mainly amphiphilic phospholipids, which are composed of a glycerol unit with two hydrophobic fatty acid “tails” and one hydrophilic phosphate ester “head group” (Figure 1A). The fatty acid tails can differ in length (normally 12–24 carbon atoms) and in their degree of unsaturation (normally zero to two *cis*-double bonds). Differences in length and saturation of the tails are important because they determine the packing of the phospholipid molecules (e.g., a double bond creates a small kink in the tail), and thus, influence the fluidity of the membrane (see below). The phos-

[a] Dr. A. Barba-Bon, M. Nilam, Dr. A. Hennig
Department of Life Sciences and Chemistry, Jacobs University Bremen
Campus Ring 1, 28759 Bremen (Germany)
E-mail: a.hennig@jacobs-university.de

 The ORCID identification numbers for the authors of this article can be found under <https://doi.org/10.1002/cbic.201900646>.

 © 2019 The Authors. Published by Wiley-VCH Verlag GmbH & Co. KGaA. This is an open access article under the terms of the Creative Commons Attribution Non-Commercial License, which permits use, distribution and reproduction in any medium, provided the original work is properly cited and is not used for commercial purposes.

phate group is mostly modified with choline, ethanolamine, or serine to provide zwitterionic phosphatidylcholine (PC) and phosphatidylethanolamine (PE), as well as negatively charged phosphatidylserine (PS) and phosphatidic acid (PA) head groups. Popular in membrane research is also the use of natural phospholipid mixtures, in particular, egg yolk phosphatidylcholine (EYPC)

In water, natural^[9] and synthetic^[10] amphiphiles can self-assemble into various supramolecular structures, such as micelles, vesicles, and inverted micelles, depending on the size and shape of the hydrophilic head group and the hydrophobic tails.^[11] Phospholipids typically form bilayer structures, in which the polar head groups of the lipids are oriented towards the surrounding water molecules and the hydrophobic hydrocarbon tails associate with each other to form an inner hydropho-

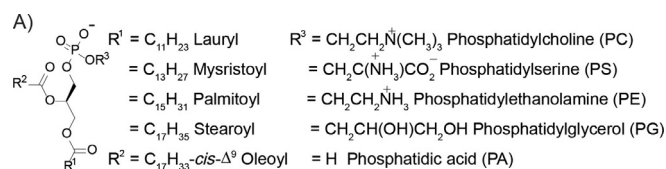
Andrea Barba-Bon graduated from the Universitat de Valencia (Spain) with a B.Sc. in chemistry in 2009 and then obtained her M.Sc. (2012) and Ph.D. (2014) degrees from the Universitat Politècnica de Valencia with research on sensors and molecular recognition. In 2015, she was awarded an Alexander-von-Humboldt Fellowship for post-doctoral research at Jacobs University Bremen (Germany). In her current research, she combines supramolecular chemistry with transport and drug delivery in biomembranes.



Mohamed Nilam graduated from the University of Colombo (Sri Lanka) with a B.Sc. in molecular biology and biochemistry. He then moved to Jacobs University Bremen (Germany) to obtain a M.Sc. in chemistry. He is currently a Ph.D. student and develops supramolecular methods to determine kinetics and activation energies of membrane permeation, as well as liposome-based supramolecular sensors.



Andreas Hennig obtained a Dipl.-Chem. from TU Braunschweig (2004) and a Ph.D. from Jacobs University Bremen (2007). After positions at the Université de Genève and the BAM Federal Institute for Materials Research and Testing, he returned to Bremen to pursue his habilitation. His goal is to design supramolecular functional systems that reliably work in complex environments, such as biofluids, membranes, and cells, as well as on nanomaterial surfaces.



| Phospholipid | R ¹ | R ² | R ³ |
|--------------|---------------------------------|---|--|
| POPC | C ₁₅ H ₃₁ | C ₁₇ H ₃₃ - <i>cis</i> - Δ^9 | CH ₂ CH ₂ N ⁺ (CH ₃) ₃ |
| DMPC | C ₁₃ H ₂₇ | C ₁₃ H ₂₇ | CH ₂ CH ₂ N ⁺ (CH ₃) ₃ |
| DPPC | C ₁₅ H ₃₁ | C ₁₅ H ₃₁ | CH ₂ CH ₂ N ⁺ (CH ₃) ₃ |
| DSPC | C ₁₇ H ₃₅ | C ₁₇ H ₃₅ | CH ₂ CH ₂ N ⁺ (CH ₃) ₃ |
| POPS | C ₁₅ H ₃₁ | C ₁₇ H ₃₃ - <i>cis</i> - Δ^9 | CH ₂ C(NH ₃)CO ₂ ⁻ |
| POPE | C ₁₅ H ₃₁ | C ₁₇ H ₃₃ - <i>cis</i> - Δ^9 | CH ₂ CH ₂ NH ₃ ⁺ |
| POPG | C ₁₅ H ₃₁ | C ₁₇ H ₃₃ - <i>cis</i> - Δ^9 | CH ₂ CH(OH)CH ₂ OH |

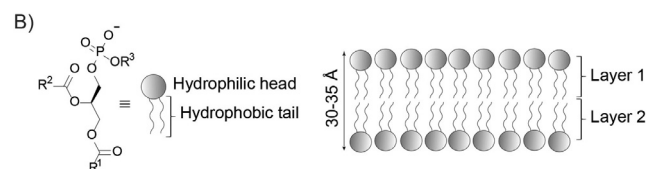


Figure 1. Structures of A) the most common phospholipids and B) the lipid bilayer membrane. POPC: 1-palmitoyl-2-oleoyl-*sn*-glycero-3-phosphocholine, DMPC: dimyristoylphosphatidylcholine, DPPC: dipalmitoylphosphatidylcholine, DSPC: 1,2-distearoyl-*sn*-glycero-3-phosphocholine, POPS: 1-palmitoyl-2-oleoyl-*sn*-glycero-3-phospho-L-serine, POPE: 1-palmitoyl-2-oleoyl-*sn*-glycero-3-phosphoethanolamine, POPG: 1-palmitoyl-2-oleoyl-*sn*-glycero-3-phospho-(1'-*rac*-glycerol).

bic layer (Figure 1 B). The center of the lipid bilayer has a polarity similar to that of hexane and is largely impermeable to hydrophilic molecules, whereas the polarity and local concentration of hydrophilic molecules increases gradually upon approaching the water–membrane interface, as elegantly mapped for micellar membranes by de Silva and co-workers.^[12] The typical thickness of the phospholipid bilayer membrane is about 30–35 Å, and the area occupied by each phospholipid molecule is about 70 Å². Values that are more accurate have been determined for numerous phospholipids and various combinations thereof, which allows the total bilayer volume, the inner vesicle volume, the interfacial surface area, and other important parameters of lipid bilayer structures to be calculated.^[13]

The self-assembled nature of the lipid bilayer membrane renders it a complex and dynamic system, which shows behavior and properties that are strongly dependent on composition and temperature (Figure 2). Typical for PC bilayers at low temperature is the gel phase, also called the solid-ordered (s_o) or L_β phase. In the gel phase, the acyl side chains of the lipids are well packed, leading to a low lateral mobility of the phospholipids, with diffusion rates of about 10^{-10} cm² s⁻¹.^[14] Upon heating, the lipids will “melt” above their phase transition temperature (T_m) and form a fluid, liquid-crystalline phase, also called the liquid-disordered (l_d) or L_α phase, with much higher lateral diffusion rates of about 10^{-7} to 10^{-8} cm² s⁻¹.^[14] Whereas the T_m value for phospholipids with unsaturated fatty acid side chains is typically too low to be practically useful to study the effects of different membrane phases (e.g., for POPC, $T_m = -2$ °C), phospholipids with saturated acyl chains are commonly used, for example, DMPC ($T_m = 24$ °C), DPPC ($T_m = 41$ °C), or DSPC

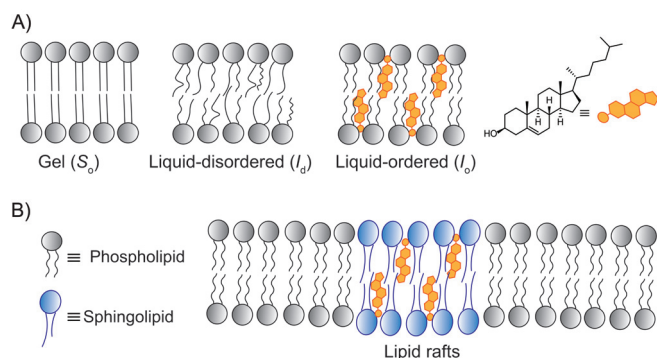


Figure 2. Schematic presentation of A) the gel phase, liquid-disordered phase, and liquid-ordered phase of phospholipid membranes, and B) membrane phase separation, leading to the formation of lipid rafts.

($T_m = 55^\circ\text{C}$). In addition to lateral diffusion within one leaflet of the bilayer, phospholipids can also undergo transverse diffusion from one leaflet to another. The rate of this “flip-flop” motion is much lower than that of lateral diffusion, with half-lives of hours to days, because the translocation of the charged head groups through the hydrophobic part of the bilayer requires a significant activation energy.

In the presence of cholesterol, a third phase forms, the liquid-ordered phase (L_o) or L_β phase. Therein, the cholesterol molecules orient themselves in the bilayer with their hydroxy groups close to the polar head groups of the phospholipid molecules, which decreases the mobility of the hydrocarbon chain in this region. Consequently, the liquid-ordered phase is less fluid than that of the liquid-disordered phase, but not as well packed as the gel phase, and diffusion rates are only moderately reduced. At high concentrations ($> 30\text{ mol}\%$), cholesterol also prevents the fatty acid tails from approaching closely and crystallizing, such that no melting of the membrane is observed and the membrane forms exclusively the liquid-ordered phase, whereas, at low cholesterol concentrations, the liquid-ordered phase coexists with the other two phases.

The coexistence of two or more membrane phases can lead to lateral phase separation within the lipid bilayer (Figure 2B). Phase-separated microdomains, also called “lipid rafts,” are well established in liposomes and the best studied model system is a ternary mixture of POPC, cholesterol, and sphingolipids (e.g., sphingomyelin). Moreover, lipid rafts are thought to play major roles in cell membranes, which are typically rich in sphingolipids and cholesterol. The rafts contain lipids with longer and straighter fatty acid chains than those of the remaining membrane lipids, which help to accumulate membrane proteins of suitable length. Lipid rafts are therefore thought to concentrate certain membrane proteins, which enables them to function together, and thus, induce key cellular processes.

2.2. Vesicles and planar lipid membranes as bilayer models

Owing to their cylindrical shape, phospholipids do not self-assemble in water in the form of spherical micelles, but prefer to form a lipid bilayer, which is flat on the molecular scale. At

larger scales, however, the bilayer rolls up to a spherical shell to seal the open ends. The resulting structures are called vesicles or, more specifically, liposomes, if they are composed of phospholipids. They separate an enclosed volume of water (the vesicle lumen) from its environment. Because phospholipid vesicles resemble empty cells, they have been extensively studied as cell membrane models and to better understand the properties of the lipid bilayer.

Another reason for the popularity of vesicles as cell membrane models is that they are relatively easy to prepare (Figure 3).^[15] Therefore, the lipids or phospholipid mixtures are

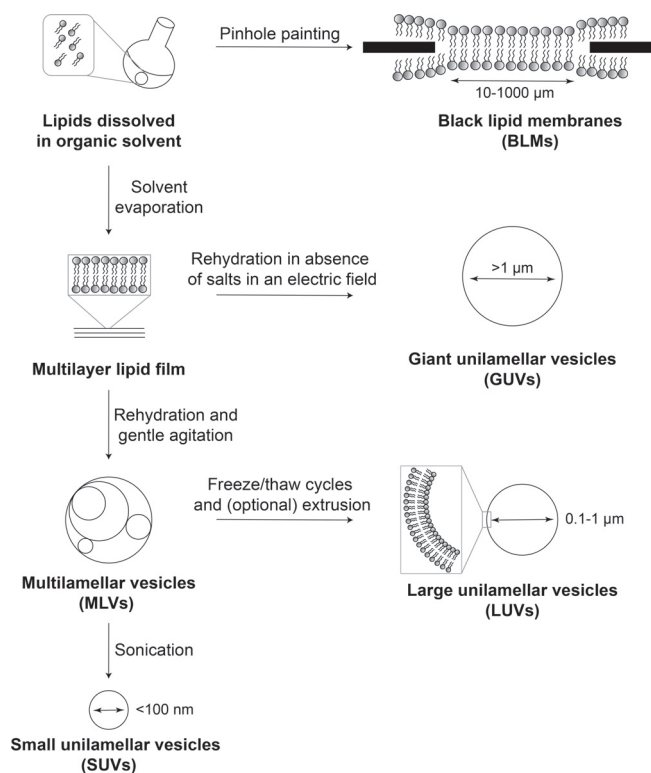


Figure 3. Vesicle preparation methods and different types of vesicles and lipid membrane models.

dissolved in an organic solvent (typically chloroform, methanol, or mixtures thereof) and the solvent is evaporated under a stream of nitrogen or by means of rotary evaporation to form a thin lipid film. Upon hydration of the lipid film by addition of water and agitation, vesicles will spontaneously form; these are typically MLVs with a broad size distribution (tens of nm to several μm). The MLVs can then be homogenized and downsized by several freeze–thaw cycles, optionally followed by extrusion of the lipid suspension through a polycarbonate membrane of defined size. The resulting vesicles are typically unilamellar and are commonly classified according to their size. Vesicles with a diameter below 100 nm are termed SUVs and vesicles with a diameter between 100 nm and 1 μm are LUVs (Figure 3). Alternative methods for the preparation of SUVs include the injection method^[16] or the dialytic detergent removal method.^[17] To encapsulate membrane-impermeable molecules in the vesicle lumen, the compounds are commonly added to

the rehydration buffer and external material is removed by means of size exclusion chromatography (SEC) after vesicle formation.

The different types of model bilayers all have experimental advantages and disadvantages. For example, LUVs are very popular due to their excellent stability, but cannot be used to study the effects of membrane curvature, for which SUVs are required. Particularly useful are GUVs, which are large enough ($> 1 \mu\text{m}$) to be directly observed by means of optical microscopy. This enabled the direct observation of lipid rafts in artificial lipid bilayer models and GUVs have also been applied to visualize membrane transport.^[18] GUVs are, however, more fragile than LUVs and may burst easily under osmotic pressure or if shear stress is applied. In addition, the removal of any extravesicular, unencapsulated material for purification is less straightforward with GUVs than that with LUVs, but may be achieved through dialysis or perfusion.^[18b,c]

Several methods have been reported for the preparation of GUVs,^[19] among which electroformation is most widely used.^[20] Therefore, phospholipids are spread on conductive indium tin oxide (ITO)-coated glass slides or platinum wires and an alternating electrical field is applied to promote GUV formation. It is well reproducible and affords relatively monodispersed and mainly unilamellar vesicles from a large number of phospholipids containing PC, PE, or PS head groups and cholesterol. An alternative is the rapid evaporation method reported by Zare and co-workers,^[21] which was, in our hands, also reliable.^[13c]

Another form of phospholipid bilayers, which has been extensively used to characterize supramolecular ion channels, are planar or BLMs (Figure 3). The BLM is formed by "painting" a lipid solution over a tiny micrometer-sized holes connecting two Teflon-coated chambers that are filled with buffer. In the absence of the lipid film, ions can freely flow through the orifice, whereas a stable lipid bilayer acts as an insulator and prevents current flow between the two electrodes. After the addition of an ion channel or pore and partitioning into the membrane, ion-channel activity is detected as a current between the two chambers. This technique is very useful to unambiguously establish whether ion transport proceeds through a carrier or pore mechanism and it is very sensitive down to the single-molecule level.

3. Membrane-Based Sensing

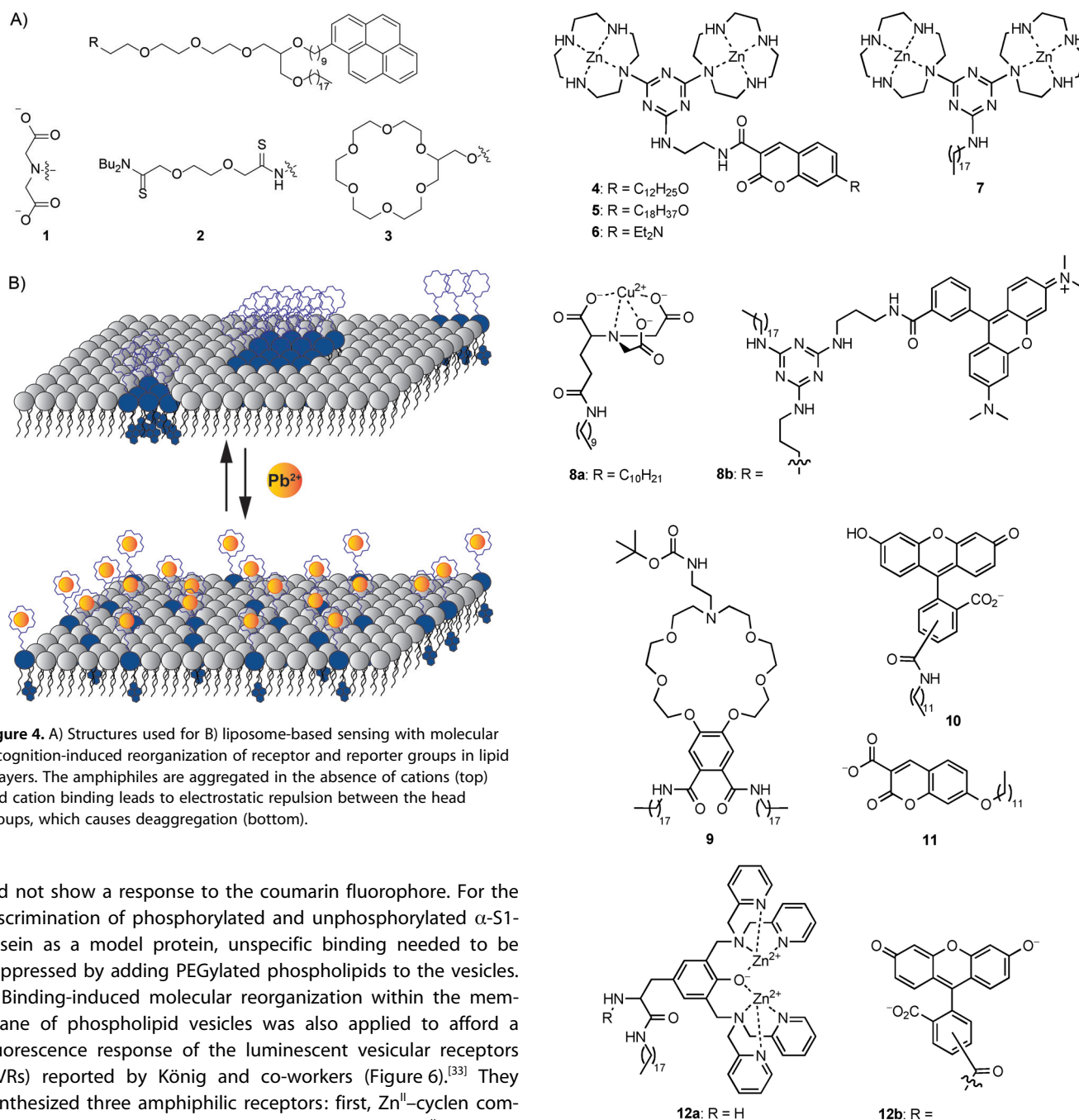
Typical supramolecular chemosensors consist of a receptor unit that acts as a molecular recognition site, a spacer, and a fluorophore or other luminescent reporter group, which converts the binding event into an optical output signal.^[22] Because the rational design and synthesis of chemosensors is often time-consuming and laborious, alternative methods have been devised. Nowadays, indicator displacement assays are very popular, in which a dye noncovalently binds to a molecular receptor and thereby changes its optical properties; subsequent addition of an analyte displaces the dye from the receptor, which restores the optical properties of the dye in solution.^[23] The commonly fast and reversible response in displacement-based chemosensors has allowed advanced versions of

indicator displacement assays for the detection of enzyme activity,^[24] membrane transport,^[18c,25] screening,^[26] reaction monitoring,^[27] and quantification of surface groups.^[28]

An alternative approach to self-assembled chemosensors is the use of monolayer and bilayer membranes, with membrane-bound amphiphilic receptor and reporter groups. This affords, similar to indicator displacement assays, a largely modular setup of different chemosensors. Most prominent is the use of poly(diacetylene) amphiphiles, which respond to binding towards coembedded receptors with a blue-to-red color change and a fluorescence increase,^[29] as well as Langmuir–Blodgett monolayers.^[30] More recently, the fluidity of the lipid bilayer membrane has been exploited for chemical sensing. Fluidity enabled a chemical recognition-induced molecular reorganization of receptor and reporter groups, which clearly distinguishes membrane-based supramolecular sensors from common strategies, in which the chemosensors are simply immobilized on solid planar or nanoparticle surfaces. Such chemosensing strategies based on the reorganization of membrane-embedded receptors and fluorophores are reviewed herein.

Early examples of metal-ion detection were reported by Sasaki and co-workers, who synthesized amphiphilic molecules containing pyrene as a fluorescent, hydrophobic group and a poly(ethylene glycol) (PEG) chain as a hydrophilic group functionalized with suitable receptors for metal-ion binding (1–3; Figure 4A).^[31] The fluorescence emission spectrum after insertion into the membrane of DSPC liposomes showed the formation of pyrene excimers, which indicated that the amphiphiles formed liquid-phase domains in the solid-phase DSPC lipid membrane. The presence of metal cations is signaled by a significant reduction of the excimer and a concomitant increase of the monomer emission. This is traced back to metal-cation binding to the receptor unit, causing electrostatic repulsion between the now positively charged head groups, which disperses the fluorescent amphiphiles (Figure 4B). Complete reversibility was shown by removal of the metal ions with ethylenediaminetetraacetic acid (EDTA). This strategy has been successfully demonstrated with iminodiacetic acid **1** as a receptor for Cu^{2+} and Fe^{3+} ,^[31a,d,e] with dithioamide **2** for Hg^{2+} ,^[31b] and with [18]crown-6 **3** for Pb^{2+} .^[31c] Notably, the authors found that the binding affinity of the iminodiacetic acid head group in **1** with various metal cations in vesicles paralleled the affinity in solution, albeit reduced by a factor of 100–1000.^[31a]

Membrane-embedded receptors carrying a fluorophore were also explored for anion sensing.^[32] König and co-workers synthesized bis- Zn^{II} cyclen complexes with a coumarin fluorophore and a dodecyl or octadecyl tail as a membrane anchor (**4** and **5**; Figure 5).^[32] If bound to a vesicle membrane, various phosphate-containing, biologically important analytes (e.g., pyrophosphate, ATP, fructose-1,6-bisphosphate, and others), including phosphorylated proteins, gave a fluorescence change, which probably originated from a local polarity change of the solvatochromic coumarin dye induced by analyte binding. As controls, receptor–dye conjugate **6**, lacking alkyl tails, was investigated in homogeneous solution. Conjugate **6** bound the analytes, as confirmed by indicator displacement assays, but



did not show a response to the coumarin fluorophore. For the discrimination of phosphorylated and unphosphorylated α -S1-casein as a model protein, unspecific binding needed to be suppressed by adding PEGylated phospholipids to the vesicles.

Binding-induced molecular reorganization within the membrane of phospholipid vesicles was also applied to afford a fluorescence response of the luminescent vesicular receptors (LVRs) reported by König and co-workers (Figure 6).^[33] They synthesized three amphiphilic receptors: first, Zn^{II}-cyclen complex **7** for the recognition of phosphate species, Cu^{II}-nitrilotriacetic acid complex **8a** for imidazole binding, and benzoaza-crown ether **9** (Figure 5) as a recognition motif for ammonium ions. If the receptors were embedded into DSPC liposomes with amphiphilic fluorescein **10** or coumarin fluorophore **11**, a significant fluorescence change was observed upon addition of analytes known to bind to the receptors. The authors speculated that, in the absence of analyte, the receptors and dyes were concentrated in mixed patches to minimize perturbations of the lipid membrane caused by the bulky amphiphiles. Binding of the analyte to the membrane-embedded receptors would change solvation and charges of the binding sites and cause the dyes to segregate from the mixed patches. This interpretation is in line with a fluorescence increase if the average distance of the fluorescein amphiphiles increases upon

Figure 5. Amphiphilic receptors, fluorophores, and fluorescent receptors, which serve as sensors, if embedded into phospholipid vesicles.

binding of pyrophosphate to the Zn^{II}-cyclen amphiphile,^[34] as well as with a fluorescence decrease of the solvatochromic coumarin-based amphiphiles upon relocation into a more hydrophilic environment. Interestingly, the affinity of the membrane-bound crown ether complex for Gly-OMe was three to four orders of magnitude higher than that expected from known solution affinities. This was ascribed to the more hydrophobic and less solvated microenvironment at the membrane-water interface.

If the concept of LVRs was extended to biomolecular aptamer receptors bound to the vesicle surface,^[35] thrombin could

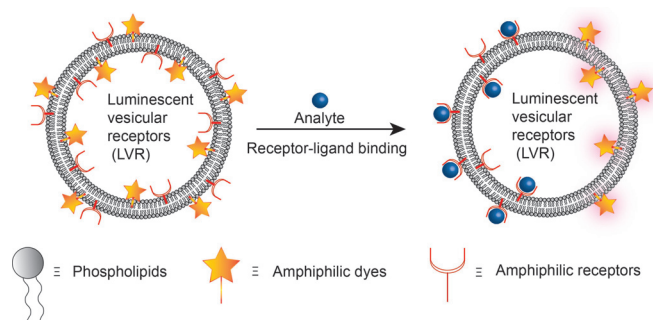


Figure 6. In LVRs, amphiphilic supramolecular receptors and dyes are co-embedded within a phospholipid bilayer membrane. Binding of an analyte (blue), leads to a spatial reorganization of receptors and dyes and a concomitant fluorescence response.

be successfully sensed with membrane-embedded rhodamine and pyrene fluorophores, but the signaling mechanism was different. Instead of a reorganization of the vesicular membrane components upon analyte binding, an aptamer-induced fluorescence quenching and regeneration of fluorescence due to conformational restrictions of the analyte-bound aptamer were presumed to be responsible for the observed fluorescence increase.

An interesting way to enhance the binding affinity between supramolecular receptors and analytes arises from the possibility of exploiting multivalent binding, in which several binding sites cooperatively interact with the desired target analyte. Classically, this requires the synthesis of covalently linked receptors. As an alternative, receptors can be immobilized on surfaces and at interfaces to display several binding sites towards a multivalent analyte or target (Figure 7). For example,

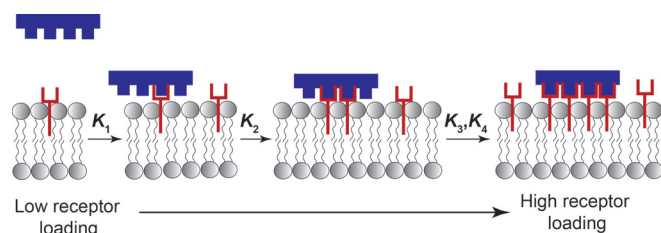


Figure 7. Binding of a multivalent ligand at vesicle interfaces and microscopic binding affinities for binding with the first surface receptor, K_1 ; second surface receptor, K_2 ; and so on.

Major and Zhu compared the binding constants of Cu^{2+} ions to surface carboxylate groups of a self-assembled monolayer of 16-mercaptohexadecanoic acid with the binding constant to succinate and glutarate in solution.^[36] The significantly enhanced binding affinity towards the surface carboxylate groups was ascribed to a “surface chelate effect,” which brings the carboxylate groups into close spatial proximity, and thus, increases their effective molarity.

An elegant model system to explore multivalent binding at phospholipid vesicle interfaces was introduced in parallel by Williams and co-workers, who investigated the binding of Cu^{2+}

to membrane-bound dansyl-labeled fluorescent lipids.^[37] Fluorescence titrations with increasing Cu^{2+} concentrations were successfully analyzed with a 4:1 (ligand/ Cu^{2+}) binding model, which indicated a significant enhancement of the binding constants compared with those in solution. However, a thorough analysis revealed that the dominant factor for the observed enhancement in binding affinity was the lower polarity experienced by the receptor at the bilayer interface and not a multivalency effect. In fact, the true binding affinity for the formation of the 2:1 ligand- Cu^{2+} complex, K_2 , was significantly lower at the membrane interface than that in solution, which was ascribed to the reduced number of degrees of freedom by constraining the receptors to the two-dimensional vesicle surface. This example clearly showed that it was hard to dissect multivalency effects from other factors that could affect binding affinities at interfaces, such as the polarity of the micro-environment, hydration effects, surface potentials, and steric crowding.

Cooperative binding at phospholipid vesicle interfaces was subsequently demonstrated by Smith and Jiang.^[38] They used a Zn^{II} -DPA (DPA: 3,5-bis[(bispyridin-2-ylmethylamino)methyl]-4-hydroxyphenyl) complex with a cholesterol membrane anchor, which was much less sensitive towards polarity effects than that of the Cu^{2+} /dansyl system, and found that ligand binding was enhanced with increasing receptor loading in the membrane. Data analysis indicated a 2:1 binding stoichiometry, and apparent binding constant K_2 clearly increased with increasing receptor loadings.

König and co-workers also tested whether bis- Zn^{II} cyclen complex **7**, which could bind to phosphoserine and histidine residues in peptides, would provide several binding sites for peptides with both residues, and thus, enhance affinity to vesicle-bound receptors.^[39] If the receptors were embedded into DSPC lipids, a relatively high receptor concentration of 10 mol% was required to observe an increased binding affinity, whereas, in DOPC lipids, a significant enhancement was already observed for only 1 mol% of receptors. This was ascribed to the fact that the DSPC vesicles were in the gel phase at room temperature (below T_m), whereas the high lateral mobility in the liquid-crystalline phase of DOPC lipids allowed a dynamic receptor reorganization, thereby increasing the affinity by more than two orders of magnitude. The same result was found for vesicles containing two different receptors, namely, Zn^{II} -DPA amphiphile **12a** (Figure 5) for phosphoserine binding and Cu^{II} -NTA (NTA: nitrilotriacetic acid) amphiphile **8a** for histidine binding.

Lateral reorganization of the amphiphiles was further confirmed by using fluorescein-labeled Zn^{II} -DPA amphiphile **12b** and rhodamine-labeled Cu^{II} -NTA amphiphile **8b** (Figure 5). In the absence of a peptide containing phosphoserine and histidine residues, the two amphiphiles showed little fluorescence resonance energy transfer (FRET). Addition of a peptide with phosphoserine and histidine residues to DOPC vesicles gave a significant increase in FRET, whereas no increase in FRET was observed in DSPC vesicles or if peptides lacking either the phosphoserine or the histidine residue were added. It has been noted that self-organization of the receptor binding sites

is reminiscent of molecular imprinting strategies, and has been termed by the authors dynamic interface imprinting. Subsequently, cross-linking of the amphiphiles was demonstrated with diacetylene-containing lipophilic tails, which were photopolymerized to afford ene-yne poly(diacetylene) polymers.^[40]

In another study,^[41] the fluorescent dyes were replaced with an amphiphilic terbium(III) complex and the receptor amphiphiles were equipped with indole as a sensitizer (also often termed antenna) that transferred energy to the Tb^{III} complex (Figure 8). A noteworthy, practical advantage of lanthanide-

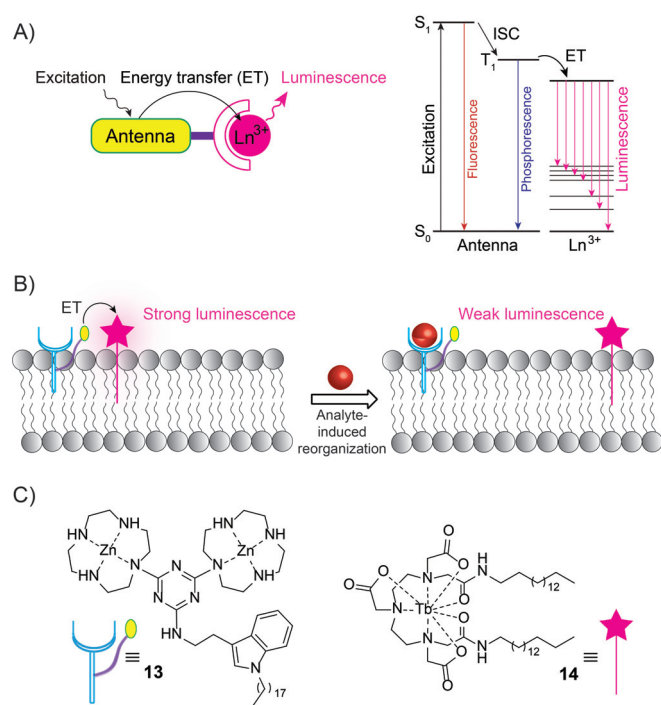


Figure 8. A) Lanthanide-based sensors require an antenna or sensitizer unit for efficient photon absorption due to the very low molar absorption coefficient of the lanthanide cations. The excitation energy of the sensitizer is transferred to the lanthanide f–f transitions after intersystem crossing (ISC) of the sensitizer. B) Lateral reorganization of membrane-bound sensitizer and lanthanide chelates modulates the energy-transfer (ET) efficiency and can be used for sensing. C) Structures of the antenna (13) and lanthanide chelate (14).

based sensors involves the long-lived emission, which can be used for nearly background-free sensing by means of time-gated detection, in which the short-lived fluorescence can be suppressed by recording the emission after a certain delay time.^[42] If receptor-sensitizer amphiphile **13** was coembedded into vesicle membranes with terbium(III) complex **14** (Figure 8C), sensitized lanthanide emission was observed upon excitation of the indole group, which decreased if phosphate-containing analytes were added. Also here, mixed patches with sensitizer and Tb^{III} in close proximity are presumably formed, which distribute after analyte binding, such that Tb^{III} sensitization becomes less efficient. Interestingly, the initial intensity of the sensor and its response depended on the type of phos-

pholipids and the lipid phase. Whereas gel-phase lipids gave a good response, a poor response was found with liquid-crystalline vesicles, which could be ascribed to two mechanisms: a less efficient assembly–redistribution of the vesicular components and an increased vibrational relaxation of the Tb^{III} complex in the liquid-crystalline phase.^[43]

4. Membrane Transport

The transport of a hydrophilic species across the hydrophobic barrier of the phospholipid membrane has long inspired supramolecular chemists to mimic this quintessential biological function. Consequently, the design of selective ion carriers, as well as membrane-spanning unimolecular or self-assembled ion channels and membrane pores, has matured into an advanced field in its own right. Because supramolecular membrane transport systems are nowadays regularly reviewed,^[8] a comprehensive treatment of this field is beyond the scope of this review and, in the following section, we focus on membrane transport systems that implement supramolecular functions in addition to “simple” membrane transport. Of particular interest are ligand-gated transport systems, in which supramolecular or biomolecular recognition principles are applied to control membrane transport activity.

The stimuli-responsive control of membrane transport across lipid bilayer membranes is a key function in cells, which is usually facilitated by sophisticated membrane proteins. The most well-known example is the opening of ligand-gated ion channels in response to biochemical messenger molecules, such as acetylcholine, which enable intercellular transmission of action potentials in synapses and thereby transduce a biochemical input into an electrical output signal. Despite the ubiquity of ligand gating in biological systems, few efforts were reported with the goal of achieving such behavior with synthetic supramolecular systems. Notably, the term “ligand gating” is an overall ill-defined process and mainly involves the function that pore activity is regulated in response towards a chemical signal.^[44] Herein, we summarize recent efforts in ligand gating of supramolecular membrane transport systems through the binding of biopolymers, metal–ligand binding, aromatic electron donor–acceptor interactions, protein–ligand interactions, and host–guest binding.

Pioneering work came from Matile and co-workers, who reported that oligo(*p*-phenylene) rigid-rod **15** could be aggregated into more active and potassium-selective π slides (Figure 9).^[45] Therefore, septi(*p*-phenylene) rods were substituted with an iminodiacetate head group, which served as a binding site for multivalent binding to poly(His) through Cu²⁺ and was known to induce aggregation of iminodiacetate-modified lipids. Aggregation of **15** in the presence of Cu²⁺ and poly(His) was confirmed by exciton-coupled circular dichroism (CD) spectroscopy, which showed a strong increase of the Cotton effect and indicated the ligand-induced formation of H aggregates. Transport experiments showed an enhanced selectivity for K⁺ transport and a switch from an Eisenman III (monomeric **15**) to Eisenman IV selectivity sequence.

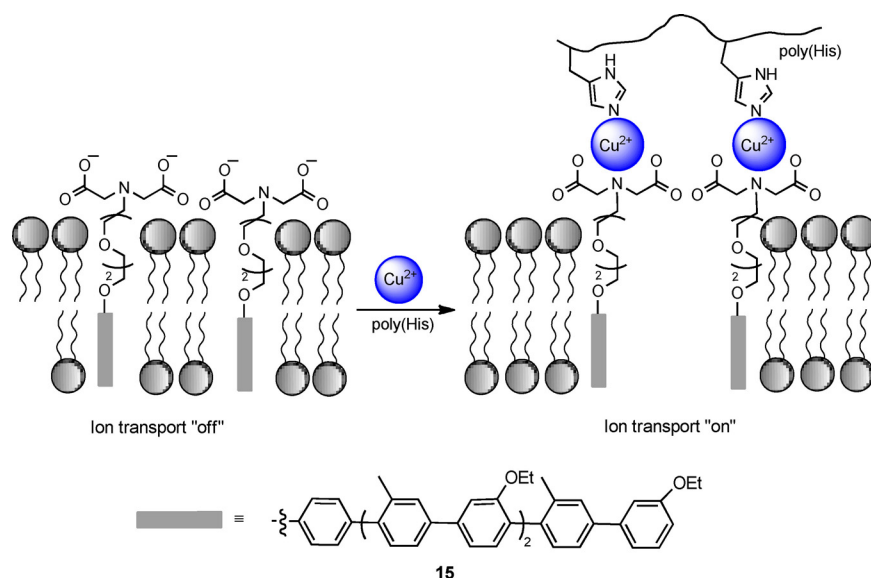


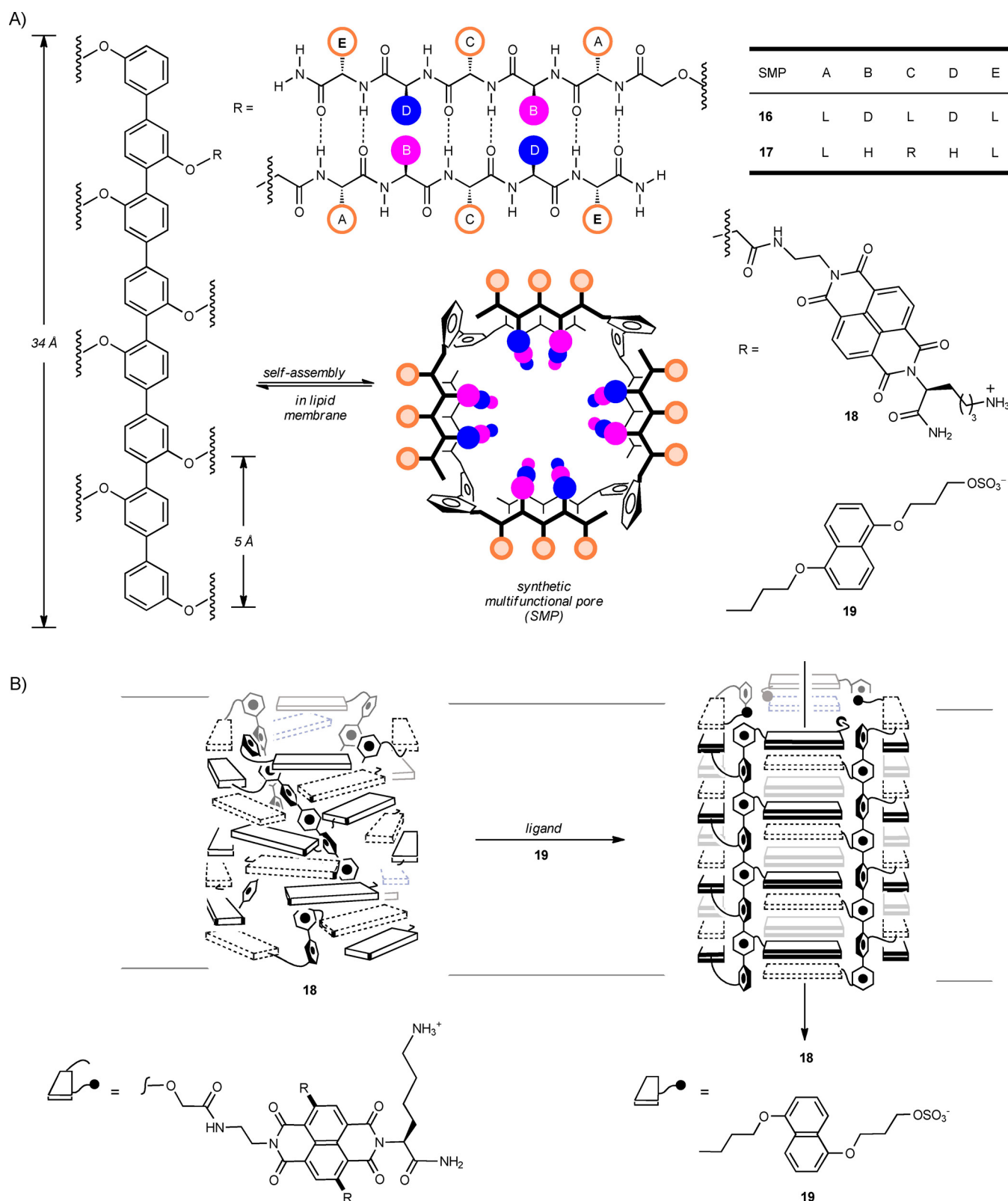
Figure 9. Self-assembly of septi(*p*-phenylene)-based rigid-rod **15** into more potassium-selective π -slide aggregates by using the binding of Cu^{2+} to the imino-diacetic acid head groups and poly(histidine) (poly(His)).

Several other examples of ligand gating from the Matile group were based on their concept of synthetic multifunctional pores (SMPs), in which octiphenyl rods, long enough to span the lipid bilayer membrane, were equipped with peptide side arms to self-assemble into tetrameric pores through the formation of β -sheets (Figure 10).^[47] The simplest examples include pore blockage of **16** with internally bound Mg^{2+} by anionic substrates and the conversion of good blockers into weak blockers and vice versa through enzymatic reactions.^[48] As another example of pore activation, the β -sheet-forming peptide arms of Matile's barrel-stave pores were equipped with Leu-Arg-Leu triads at the outer surface to afford **17**.^[49] The presence of the hydrophilic, external arginine residue prevented efficient membrane partitioning, but scavenging of amphiphilic counteranions by the external arginine residues rendered the pore more hydrophobic, such that it could insert into the membrane and cause efflux through the pore.

A very elegant design involved conformational switching of a π -stacked architecture of aromatic electron donors and acceptors in SMPs.^[46,50] Therein, the peptide side arms of the pores were replaced by naphthalenediimides (NDIs) to give **18**, which self-assembled into twisted π helices in the lipid bilayer, as indicated by their CD spectra because of the mismatch between the repeat distance of π -stacked aromatic surfaces (3.4 Å) and the repeat distance at the attachment sites at the octiphenyl rods (5 Å). Reminiscent of a diaphragm shutter, the shortened distance of the twisted π stacks closes the central hole through which exchange proceeds. Addition of DAN **19** gave alternating DAN/NDI stacks by means of DAN intercalation, as indicated by the appearance of a charge-transfer band in the absorption spectra and CD silencing, which indicated a parallel arrangement of the NDI transition dipole moments in the intercalated structure. This is in agreement with a cooperative untwisting to afford an open membrane pore.

The use of metal–ligand interactions to assemble supramolecular ion channels and pores inside lipid bilayers was shown by Webb and co-workers with Pd^{II} .^[51] They synthesized pyridyl cholates conjugates **20–22**, which were long enough to match the thickness of one leaflet of the lipid bilayer (Figure 11 A). According to their concept, the addition of PdCl_2 to **20** connects two pyridyl groups, leading to the formation of a dimer, which is then long enough to span the lipid bilayer membrane and afford Na^+ -selective ion transport (Figure 11 B). The addition of hexathia[18]crown-6 as a strongly chelating ligand for Pd^{2+} removes palladium from the pyridyl groups, leading to disassembly of the ion channel. This demonstrated the full reversibility of Pd^{2+} gating, which was further corroborated by alternating additions of Pd^{2+} and crown ether. Interestingly, the in situ combination of PdCl_2 and monomer should give initially the (presumably inactive) *cis* isomer, which converts into the thermodynamically more stable (and active) *trans* isomer within minutes. A corresponding lag phase in the recorded fluorescence traces was, however, not observed, and a pre-equilibrated *trans* product was found to be less active than that of the in situ mixture. That the active species is the kinetically favored *cis* isomer is, however, also unlikely because a *cis*-Pt complex of the pyridyl cholates is inactive.

The pyridyl cholates system was further modified with biotin groups to afford **21**, which enabled the system to undergo additional levels of supramolecular assembly through biotin–avidin binding.^[52] The PEG chain was introduced to provide sufficient flexibility in the linker and, thus, prevent any unfavorable steric effects in the binding of biotin to the comparably deep binding pocket of avidin. Binding of the biotin group to the tetravalent avidin protein should modulate the lateral assembly of two or more membrane-spanning Pd pyridyl cholates complexes into active pores (Figure 11 C). It was found that the ion-transport activity assessed by a liposome-based fluores-



cence assay decreased in the presence of avidin, which could result from preventing the lateral assembly at the right dis-

tance for ion transport, from blocking the pore entrance or from vertically displacing the pores in the membrane to render

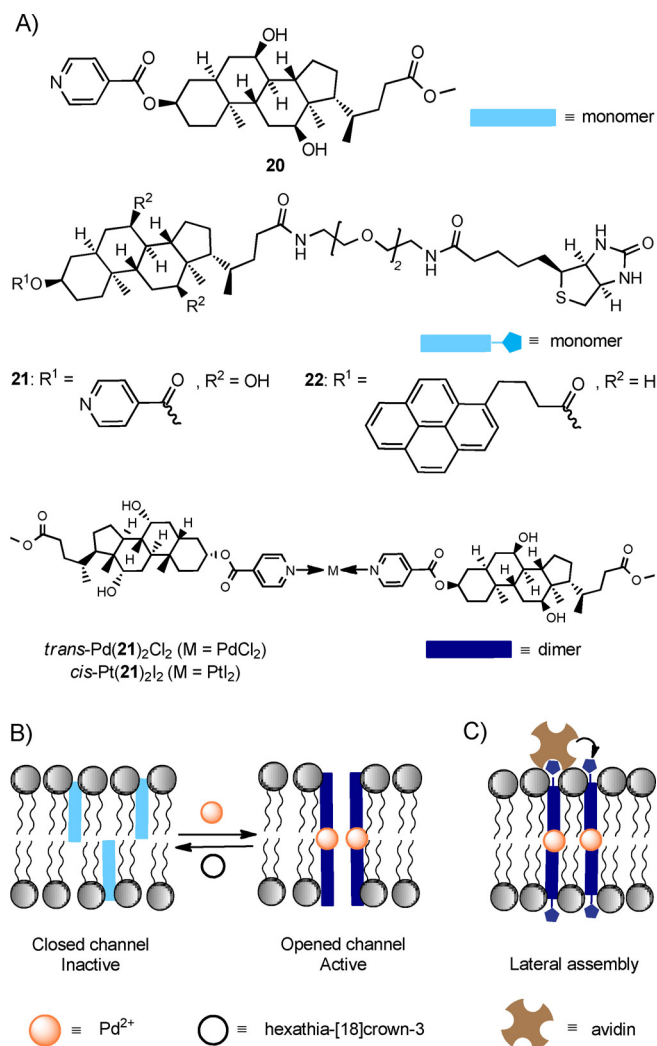


Figure 11. A) Pyridyl cholate conjugates for Pd^{II}-mediated ligand gating. B) Formation of dimers of **20** and Pd^{II} to afford open Na⁺-selective ion channels. C) Lateral self-assembly of pyridyl cholate conjugates **21** equipped with biotin head groups by addition of tetrameric avidin.

them inactive. Conductance measurements in planar lipid bilayers demonstrated that channel openings became less frequent in the presence of avidin, which indicated that avidin inhibited pore formation. To provide more insight into the inhibition mechanism, pyrene-labeled derivative **22** was used, and an increase in the excimer-to-monomer emission ratio was observed upon the addition of avidin, which suggested that pore blocking, rather than preventing lateral assembly, was the reason for a reduced transport rate. It may be argued that the distance between two biotin-binding pockets on avidin is too large (30 Å) to efficiently assemble the channels, but the ideal distance for excimer formation is much shorter (ca. 8 Å); this indicates sufficient flexibility of the avidin-bound channels.

In a parallel work, Webb and co-workers synthesized bis-5,15-(*meso*-3-pyridyl)porphyrin **23**, which was long enough to span the lipid bilayer membrane and self-assemble into various oligomers in the presence of Pd^{II} in solution.^[53] Transport experiments indeed showed dye efflux from carboxyfluorescein (CF)-loaded vesicles, but not from vesicles containing fluores-

cein isothiocyanate–dextran. This suggested that some of the oligomers might represent supramolecular boxes with cavities large enough to allow transport of species larger than that of metal ions (Figure 12). The dominant species in the mixture was supposed to be a cyclic trimer. It matched the coordination geometry of Pd^{II} and the porphyrin, and the authors could obtain indirect evidence that the trimer was most likely to be the transport-active species.

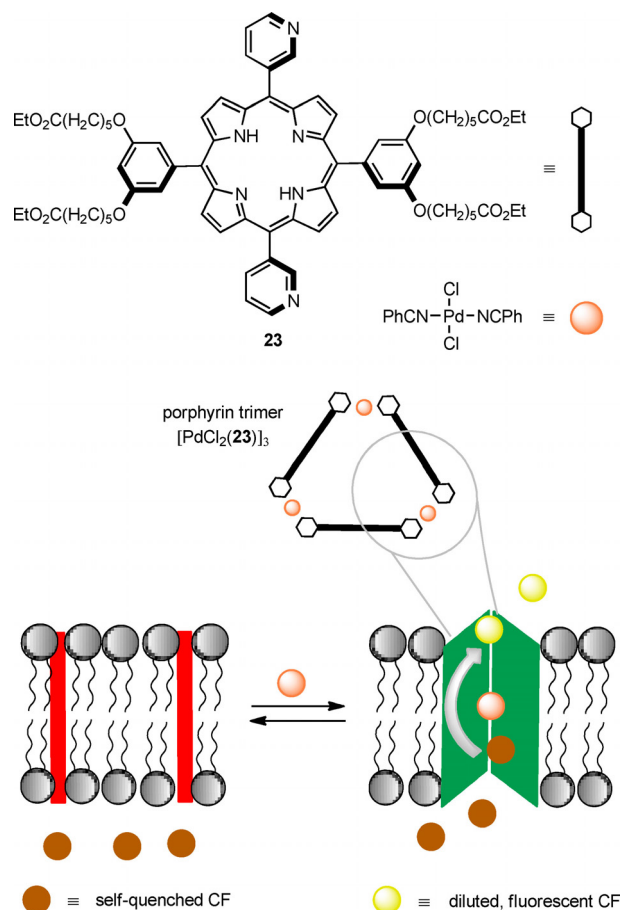


Figure 12. Porphyrin **23** self-assembles into membrane-spanning Pd^{II}-porphyrin trimers, which afford membrane pores sufficiently large enough to release self-quenched CF from phospholipid vesicles.

Nitschke and co-workers recently reported metal–organic-ion channel **24**, which was obtained by subcomponent self-assembly of 10 Zn²⁺ ions and 15 ligands (Figure 13).^[54] The pentagonal-prismatic Zn₁₀L₁₅ complex has a central cavity with a diameter of about 2.3 Å, which is large enough to accommodate anions, as observed in the X-ray crystal structure. It was shown that **24** inserted into lipid bilayers, and ion current measurements and fluorescence assays performed with BLMs and LUVs were consistent with halide transport through the bilayer membrane. Ligand gating was also demonstrated by using dodecyl sulfate as an efficient blocker.

Ligand gating based on host–guest complexation has also been reported for calixarenes. Li and Chen reported that the parent, unsubstituted calix[6]arene (CX6) acted as an efficient

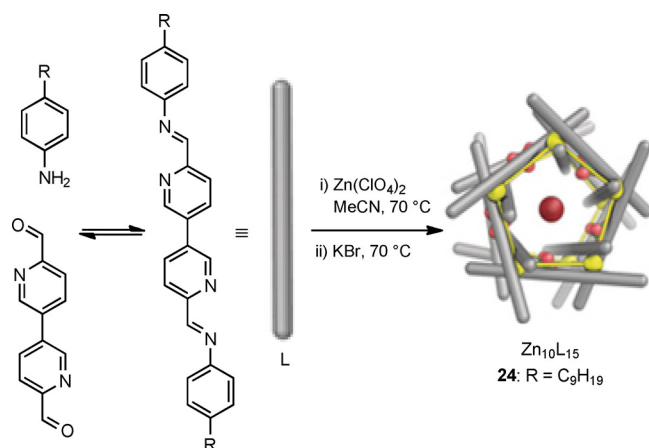


Figure 13. Ion channel **24** was obtained by means of subcomponent self-assembly and transported halide anions across lipid bilayers through the central cavity. The latter could be blocked by dodecyl sulfate. Adapted with permission from ref. [54]. Copyright: 2017, Wiley-VCH.

ion channel, as shown by means of 8-hydroxypyrene-1,3,6-trisulfonate (HPTS) assay and conductivity measurements.^[55] Ion transport by CX6 could be blocked by the addition of methylene blue as an established cavity binder. In the presence of the water-soluble *p*-sulfonatocalix[6]arene, which binds methylene blue more strongly than that of the parent CX6, blocking could be reversed through a host-exchange reaction.

Another example of ligand gating was reported by Kinbara and co-workers.^[56] From combined CD spectroscopy, fluorescence depth quenching, and Langmuir–Blodgett measurements, the authors inferred that diphenylacetylene-based bolaamphiphile **25** inserted into lipid bilayers and adopted an “M”-shaped conformation (Figure 14). In the proposed structure, the two diphenylacetylene groups are located in the membrane, the octaethyleneglycol chains extend into the aqueous phase, and the tris(isopropylsilyl) groups are close to the bilayer surface. Although **25** itself did not afford transport across lipid bilayers, the addition of phenethylamine to both chambers in BLM measurements gave an increase in the current flow in single-channel measurements, in accordance with the ligand-templated formation of a self-assembled supramolecular ion channel. Subsequent addition of β -CD, which is a known host for phenethylamine, led to a reduction of the ion current; this suggested host-induced disassembly of the ion channel. The ion-channel current could subsequently be turned on again by further addition of phenethylamine, thereby demonstrating the excellent, reversible ligand gating of the channel.

Because cyclodextrins are well known to bind hydrophobic molecules, and thus, extract them from a lipid bilayer membrane, the activity of chloride carrier **26** could also be turned off by the addition of β -CD (Figure 15).^[57] The adamantane groups are a well-established binding motif for β -CD and the formation of a 2:1 host–guest complex almost completely shut off the transport activity of **26**. Subsequent addition of a competitive binder displaced **26** from β -CD, which could then re-partition into the membrane to turn on chloride transport.

Selective host–guest complexation of membrane-embedded amphiphilic *p*-sulfonatocalix[4]arene **27** was recently estab-

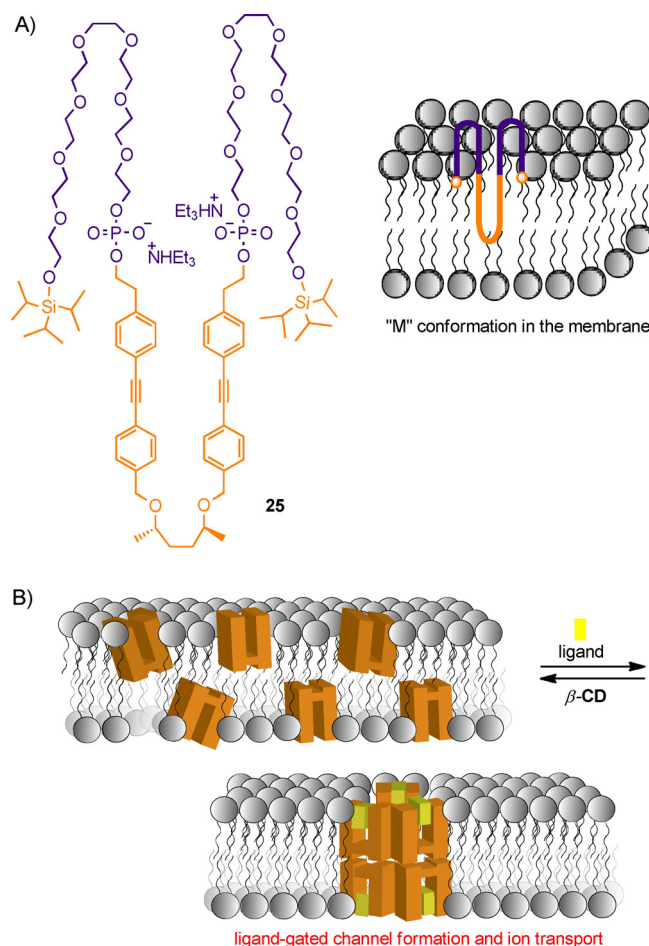


Figure 14. A) Bolaamphiphile **25** inserts into lipid bilayers and adopts an M-shaped conformation in the lipid membrane. B) In the presence of phenethylamine, ion channels are formed, whereas β -cyclodextrin (β -CD) can extract the ligand from the membrane, leading to channel disassembly.

lished by us for enzyme-regulated ligand gating of membrane transport (Figure 16).^[18c,58] We found that nanomolar concentrations of **27** efficiently transported cell-penetrating peptides (CPPs) and other cationic peptides across phosphocholine membrane by host–guest formation at the membrane interface, partitioning of the complex into the membrane, and peptide release into the vesicle lumen. We could show that the overall transport efficiency was largely determined by the affinity of the peptide to the calixarene. This enabled the selective transport of kinase substrates P1 and P2, whereas transport was shut off during peptide phosphorylation by protein kinase A (PKA) or protein kinase C (PKC). Notably, the enzyme-mediated regulation of supramolecular membrane transport activity affords, in conjunction with fluorescence monitoring, label-free enzyme assays.^[48,58,59] Such label-free kinase assays are highly sought-after in drug discovery by means of high-throughput screening.^[24e,42c]

5. Artificial Signal Transduction

To sense and respond to environmental changes, cells must be able to convert the change in extracellular conditions into a

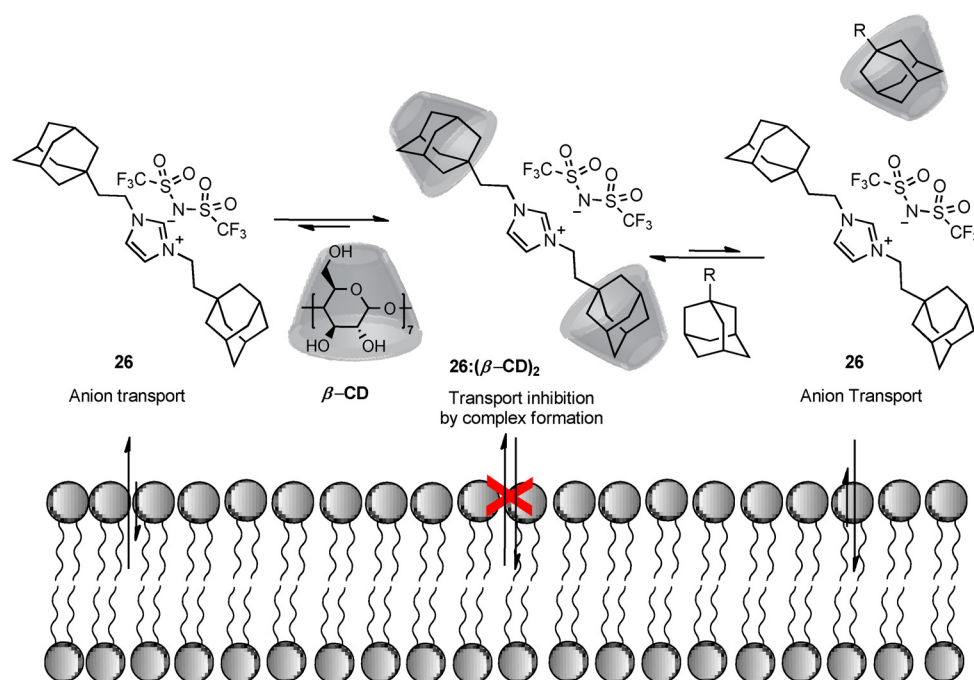


Figure 15. Bis(adamantane)imidazolium **26** acts as an efficient chloride anion carrier in lipid vesicles. Addition of β -CD extracts **26** from the membrane and thereby shuts off membrane transport.

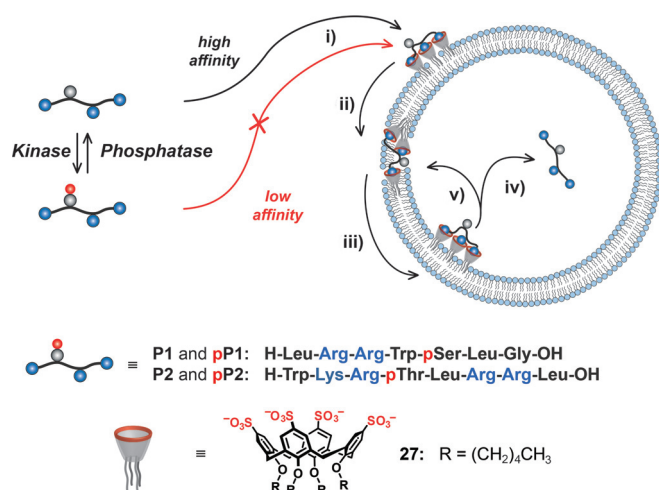


Figure 16. Phosphorylation-responsive membrane transport of peptides P1 and P2 by amphiphilic calixarene **27**. The reduced affinity of the phosphorylated peptides for membrane-bound calixarene **27** prevents i) binding and charge neutralization, such that ii) membrane partitioning, iii) translocation, and iv) release or v) shuttling back are only possible with unphosphorylated peptides. Adapted with permission from ref. [58]. Copyright: 2017, Wiley-VCH.

functional change inside the cell. In addition to gating of membrane transport processes, in which chemical signals are physically exchanged between the inner and outer compartments of a cell or vesicle, signal transduction across lipid bilayers can also be achieved without the transport of molecules. Prototypical examples in live cells are membrane-spanning G protein-coupled receptors (GPCRs) and tyrosine kinases, in

which binding of an extracellular ligand leads to protein dimerization and subsequent activation of intracellular protein domains that exert an intracellular enzyme activity. Supramolecular chemists have so far explored artificial transmembrane signaling systems, in which an external chemical stimulus induces an intravesicular reaction or light emission. Therein, two design principles were devised: lateral receptor dimerization reminiscent of GPCRs and stimuli-induced transversal movement and translocation of a membrane-bound signaling unit.

5.1. Receptor dimerization

The first report on an artificial transmembrane signaling system dates back to the early 2000s.^[60] Therein, tail-to-tail cholesterol dimers were synthesized from propargyl esters of cholenic acid through a Glaser–Hay coupling and subsequently equipped with cysteine, which was then reacted with 2,2'-di-pyridyl disulfide to afford a pyridine-2-thiol disulfide at none (**28**), both (**29**), or one head group (**30**) of the membrane-spanning molecule (Figure 17). The key idea is to prepare a membrane-embedded mixture of **28** and **30**, in which the latter has its disulfide exclusively oriented towards the vesicle interior. The intermolecular reaction between **28** and **30** to release yellow-colored pyridine-2-thiol is supposed to proceed very slowly, whereas disulfide formation at the outer leaflet by oxidation brings the disulfide and thiol on the inner leaflet into close proximity, leading to a pronounced increase in reaction rate. Notably, disulfide exchange, which is also very popular in dynamic combinatorial chemistry,^[61] has been extensively exploited by Regen and co-workers in lipid membranes to map the lateral organization of lipid bilayers,^[62] to address the mysterious mechanism of action of general anesthetics, such as

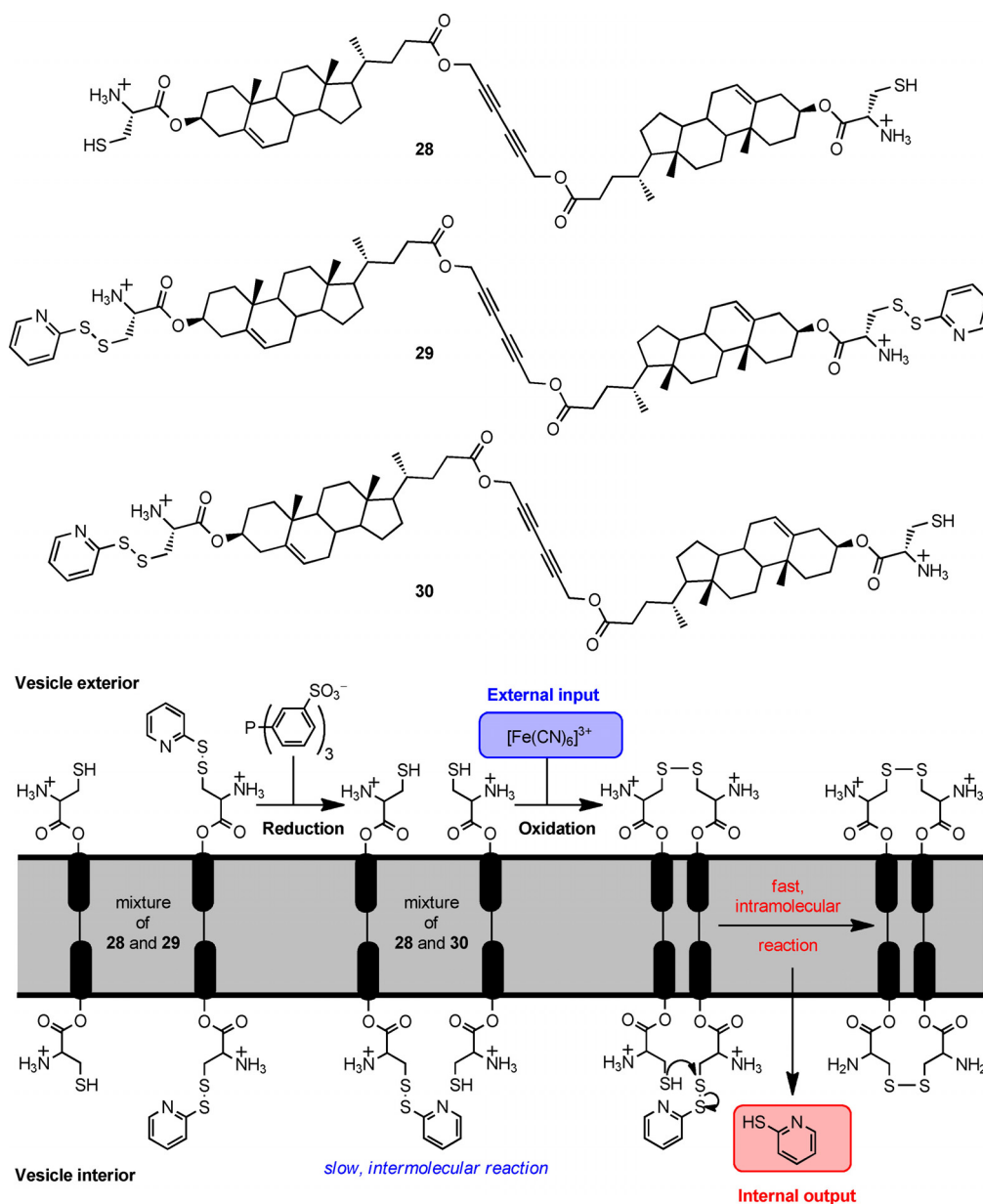


Figure 17. Artificial transmembrane signaling, in which oxidation of the thiol groups induces dimerization by disulfide formation and thereby increases the rate of intravesicular pyridine-2-thiol release from a slow intermolecular to a fast intramolecular reaction.

chloroform,^[63] and to shine light on the driving forces of lipid raft formation.^[64]

To afford the desired asymmetric orientation of **30** in the lipid bilayer, compound **29** was used in the preparation of the vesicle and external disulfide was removed by the addition of tris(3-sulfonatophenyl)phosphane, which was a charged, and thus, membrane-impermeable reducing agent. This affords membrane-bound **30**, in which all disulfide units are located on the inside of the vesicles. Subsequent addition of the oxidant potassium ferricyanide gives the intermolecular disulfide between **28** and **30** at the outer leaflet, which is signaled by an increase in the UV/Vis absorption at $\lambda \approx 341$ nm and indicative of the intravesicular release of pyridine-2-thiol.

In a subsequent extension of this work, tail-to-tail dimers of cholesterol were equipped with fluorescent dansyl ethylenedi-

amine head groups, which acted as binding sites for copper(II) ions and induced oligomerization of receptor **31** (Figure 18).^[65] If Cu^{2+} was externally added to vesicles containing the dansylated cholesterol dimers, fluorescence quenching was observed in a Cu^{2+} -concentration-dependent manner that was indicative of Cu^{2+} binding. Notably, Cu^{2+} ions readily cross the lipid bilayer, leading to an equilibration of internal and external Cu^{2+} concentration within about 30 min, such that the intravesicular binding sites are also occupied after this period.

If the results from the membrane-spanning cholenic acid dimer were compared with the cholesterol monomer **32**, which could only occupy half of the lipid bilayer, it was noted that less Cu^{2+} was required for the dimer to afford the same level of fluorescence quenching as that for the monomer. This result suggests that receptor clustering in the case of the

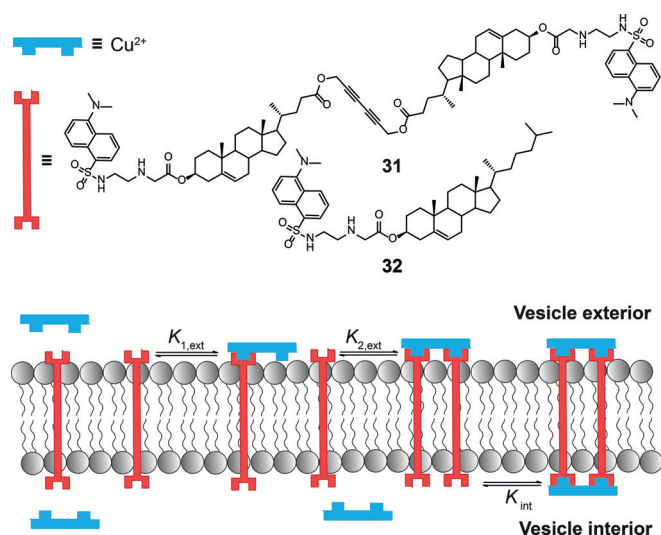


Figure 18. Cooperative binding at the inner leaflet after receptor clustering induced by the external addition of Cu^{2+} .

dimer facilitates Cu^{2+} binding at the inner membrane leaflet. The cooperative binding of the second Cu^{2+} at the inner leaflet is thus enhanced by the spatial preorganization of several receptor molecules affected by binding of the first Cu^{2+} at the outer leaflet, leading to an increased effective molarity. The work thus demonstrates how an extravesicular binding event can preorganize a second binding site intravesicularly.

A related system was also synthesized and explored by Schrader and co-workers, in which they replaced cholenic acid

with lithocholic acid and the dansyl ethylenediamine head groups with *m*-xylene bisphosphonate (**33**) and boronic acid (**34**) head groups (Figure 19).^[66] The goal was to use adrenaline as an external messenger molecule, which could form a boronate ester with its catechol group and bind to the bisphosphonate with its secondary ammonium group. This would bring the thiol and pyridine-2-thiol disulfide into close proximity to enable the adrenaline-triggered release of pyridine-2-thiol. Unfortunately, the envisaged signal transduction event did not take place. This was ascribed to a noncovalent interaction between both transmembrane units, involving the formation of a boron–nitrogen bond and a bisphosphonate ammonium ion pair, which prevented efficient binding of the adrenaline messenger.

Signal transduction was, however, observed in a slightly different experimental setup, in which a combination of transmembrane units **33** and **35** responded to the addition of diethylenetriamine as an extravesicular messenger with the release of pyridine-2-thiol.^[67] Interestingly, the functionality of the system largely depended on the lipid composition of the vesicles. EYPC was fully incompatible with the signal transduction system and the addition of diethylenetriamine led to vesicle precipitation. If mixtures of DPPC and DMPC were explored, a strong dependence on the lipid membrane fluidity was noted. In pure DMPC vesicles, the background reaction was comparably high, which was ascribed to the high fluidity of this membrane, whereas, in pure DPPC, both the background reaction and signal generation were low. The optimal lipid mixture was 3:1 DMPC/DPPC, in which a good compromise between the background reaction and signal generation was

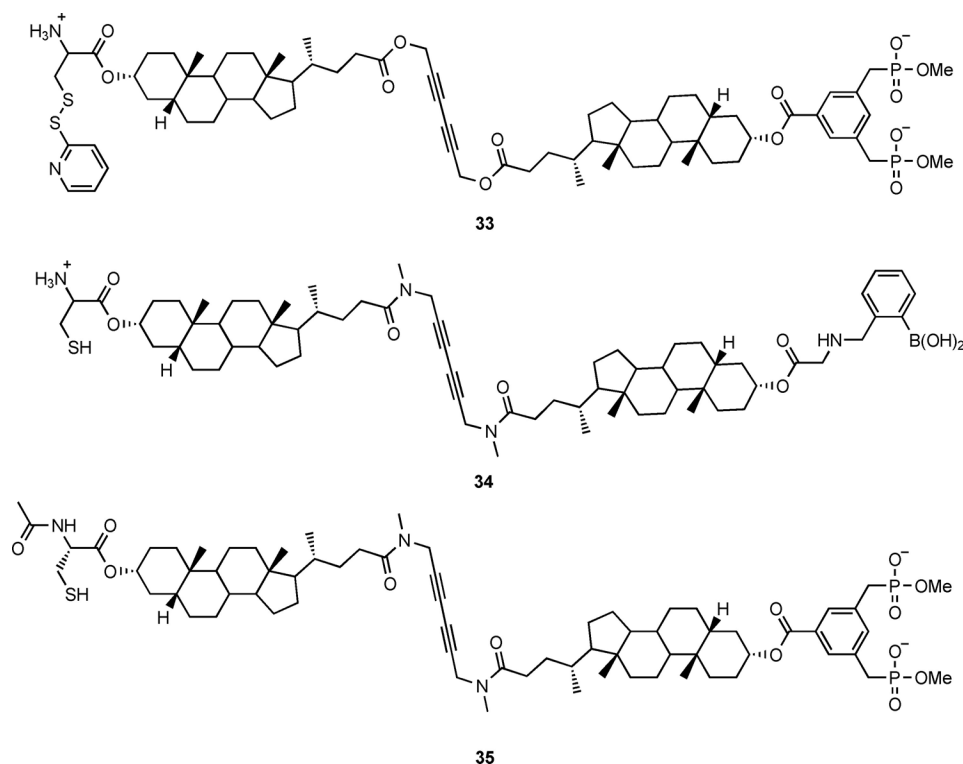


Figure 19. Lithocholic acid based membrane receptors **33**–**35**. Liposomes with **33** and **34** were explored for adrenalin binding and liposomes containing **33** and **35** responded to the addition of diethylenetriamine as an extravesicular messenger by release of pyridine-2-thiol (cf. Figure 17).

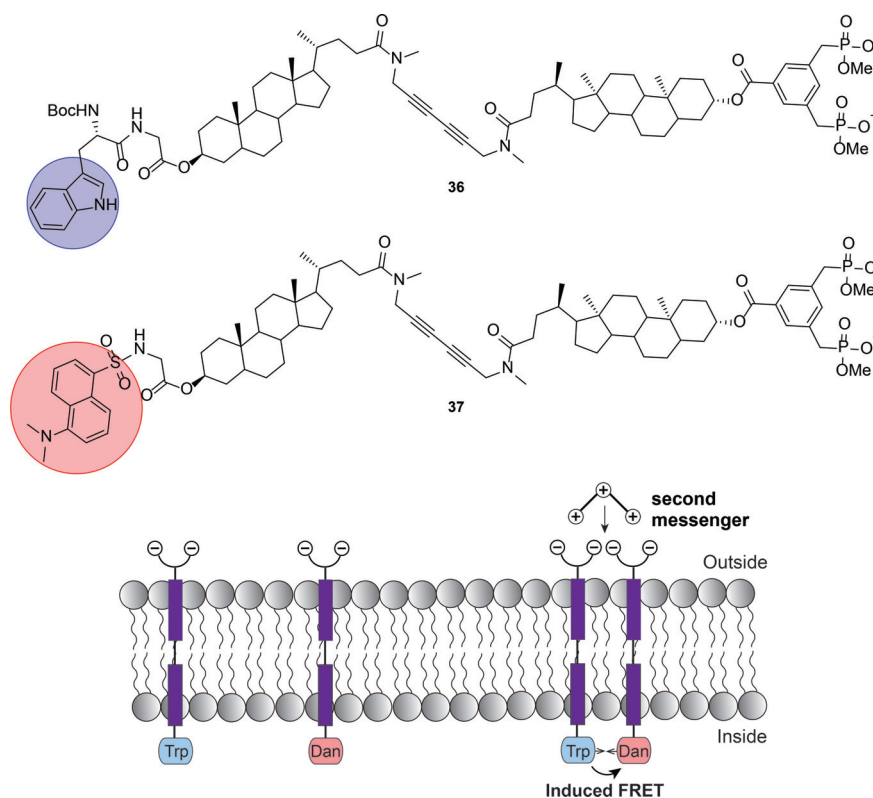


Figure 20. FRET as an output signal for transmembrane signaling. An externally added messenger (diethylenetriamine) induces heterodimerization of membrane-embedded **36** and **37**; brings them into close proximity; and, thus, enables FRET between the indole group of tryptophan (Trp) and the dansyl (Dan) fluorophore. Boc: *tert*-butyloxycarbonyl.

found. Interestingly, other polycations, such as spermine, spermidine, oligolysine, or oligoarginine, gave no signal, presumably because the distance between the thiol and disulfide groups was too large with these molecules.

As an alternative to a chemical output signal, FRET on the intravesicular membrane has also been demonstrated (Figure 20).^[68] Therefore, the transmembrane units were synthesized with *m*-xylene bis-phosphonate head groups and a tryptophan FRET donor (**36**) and a dansyl acceptor (**37**) at the other end. Incorporation of both transmembrane units into DPPC vesicles gave a moderate FRET signal in the absence of an external messenger, which increased upon the addition of an excess of diethylenetriamine. The overall response was, however, not very large because not all bis-phosphonate head groups were oriented outwards, and thus, only a fraction could bind the messenger molecule. Moreover, receptor clustering will also give donor/donor and acceptor/acceptor dimers in addition to the desired donor/acceptor dimers, which further diminishes the maximum achievable FRET signal. Nonetheless, an optimal balance between background FRET and signal was achieved with a 3:1 mixture of DMPC/DPPC, which showed a 25% decrease in tryptophan and a 30% increase in dansyl emission intensity upon the addition of a messenger.

A potential U-shaped conformation of the transmembrane units was readily excluded by extravesicular addition of eosin as an additional FRET acceptor to afford a multi-FRET system. In the absence of a messenger, both dansyl and tryptophan emis-

sions were reduced and the fluorescence from eosin was increased; this indicated the association of eosin with the outer membrane leaflet or with outer dansyl chromophores. If the external messenger was added, FRET from tryptophan to dansyl increased, whereas the fluorescence from eosin remained unchanged. This clearly demonstrated that the transmembrane units indeed adopted a transmembrane orientation; in the case of U-shaped transmembrane units, an enhanced multi-FRET effect would be otherwise expected. An additional benefit of the multi-FRET system was that it gave a visible color change to enable the naked-eye detection of the signal transduction event.

5.2. Catalyst translocation

As shown in the previous section, signal transduction without the physical exchange of the inner and outer compartments of the vesicles has proven to be a significant challenge. Even less explored is the possibility to activate a catalyst in the inner compartment of a vesicle upon extravesicular signal generation. The activation of intracellular enzyme reaction cascades presents the most common signal transduction mechanisms in biology. In addition, catalysis affords not only signal transduction, but also signal amplification because binding of a single molecule can generate a large number of output molecules.

A genuinely artificial system for activating a catalyst on the intravesicular side of a vesicle membrane has been recently introduced by the groups of Williams and Hunter.^[69] They func-

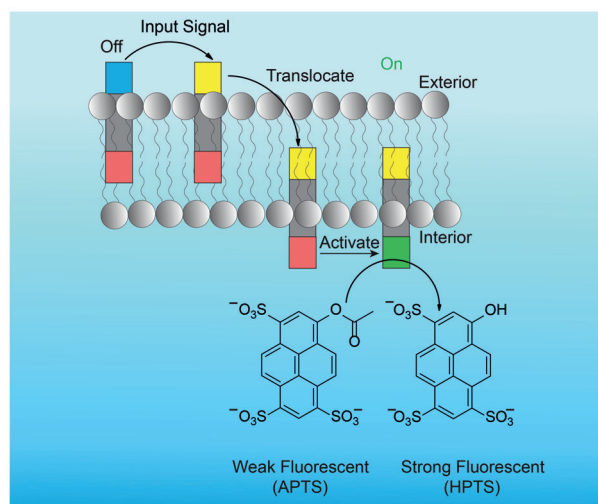
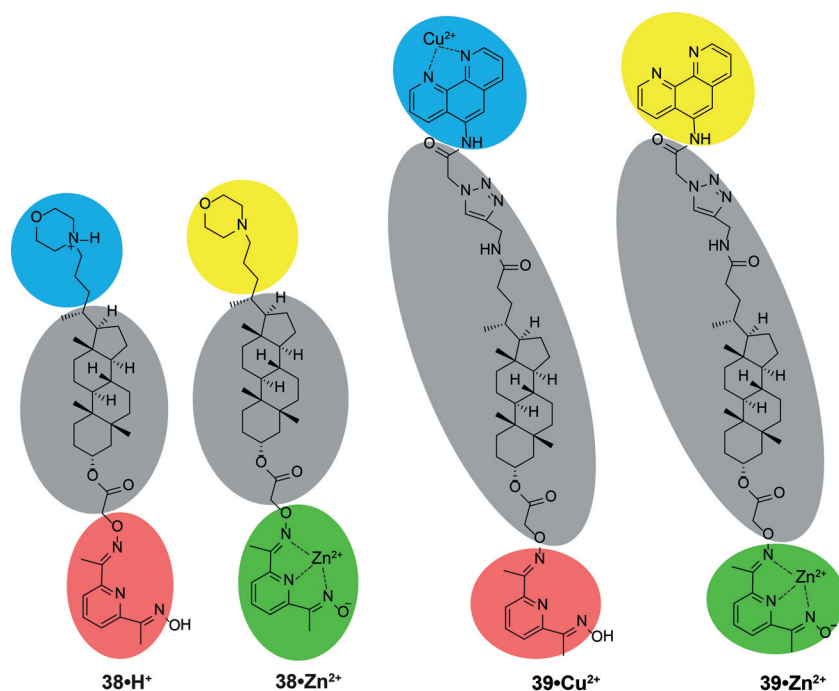


Figure 21. Artificial transmembrane signal transduction by transversal movement of **38·H⁺** after deprotonation of the morpholine head group or of **39·Cu²⁺** after the removal of Cu^{2+} by EDTA. At the inner leaflet, binding of intravesicular Zn^{2+} to the pyridine oxime group gives the active catalysts **38·Zn²⁺** or **39·Zn²⁺** that catalyze the hydrolysis of fluorogenic 8-acetoxypyrene-1,3,6-trisulfonate (APTS) into fluorescent HPTS.

tionalized lithocholic acid with a morpholine group at one end and a pyridine oxime as a procatalyst at the other end to afford **38** (Figure 21).^[69a] Overall, the molecule is too short to span the lipid bilayer, such that either the morpholine group or the pyridine oxime group is positioned at the outer membrane–water interface. The idea is that the protonated morpholinium ion in **38·H⁺** will position the morpholine head group at the interface and the procatalyst at the center of the lipid bilayer, whereas a base pulse will deprotonate the morpholinium ion and allow the catalysts to shuttle to the other side of the membrane. On the inner leaflet, a Zn^{2+} is bound by the pyridine oxime and converts the procatalyst into its active form, **38·Zn²⁺**. The catalytic activity of **38·Zn²⁺** was signaled by hydrolysis of nonfluorescent APTS into fluorescent HPTS. Re-

versible switching of the signal transduction activity was also shown by repeated deprotonation/reprotonation cycles. Notably, vesicles could be conveniently prepared with a statistical distribution of **38**, in which half of the transducer population had its recognition group positioned into the vesicle interior. However, only transducer molecules with an outwardly oriented recognition group will generate a signal, because intravesicular pH 7 locks the protonated morpholinium ion at the intravesicular membrane–water interface.

Subsequently, in **39**, the morpholine head group was replaced by a phenanthroline (phen) group for copper(II) binding.^[69b] If copper is bound to phen, the lipid head group becomes charged and is thus locked at the membrane interface of the outer membrane leaflet. Extravesicular addition of EDTA

as a competitive binder for Cu^{2+} converts the hydrophilic $[\text{Cu}(\text{phen})]^{2+}$ complex into a hydrophobic phen head group, which can then shuttle towards the internal membrane leaflet and form the active catalyst. Also, here 39-Zn^{2+} converted APTS into HPTS and reversible switching could be demonstrated by repeated addition of EDTA and Cu^{2+} . To unambiguously establish the actual compartmentalization of the signal transduction system, the experiment was repeated after external addition of the quencher *p*-xylene-bis-pyridinium bromide (DPX). Identical final fluorescence intensities after hydrolysis of APTS into HPTS in the absence and presence of external DPX clearly demonstrated that catalyzed ester hydrolysis proceeded exclusively in the vesicle lumen.

It is interesting to note that the membrane orientation and positioning of the transducer could be elegantly controlled by different affinities of Cu^{2+} and Zn^{2+} to the two different binding sites. Because the copper–phen complex has a much higher affinity ($\log K=9.0$) than that of the zinc-2,6-diacetylpyridine dioxime complex ($\log K=4.6$), the copper–phen complex is exclusively formed if vesicles are prepared in the presence of equimolar amounts of transducer and Cu^{2+} , and an excess of Zn^{2+} . This affords a statistical distribution of transducer molecules, in which half of the population is oriented with the copper–phen complex inwards and the other half outwards of the vesicle. Whereas the inward-oriented transducers remain inactive upon the addition of membrane-impermeable EDTA, the outward-oriented transducers can shuttle to the inside because EDTA binding is even stronger and removes external Cu^{2+} .

It would be interesting to see whether signal transduction still proceeded, if the vesicles were prepared with an excess of internal Cu^{2+} : assuming an exclusive shuttling motion of the transducer would still give a signal transduction event, whereas a flipping motion of the transducer would orient the phen group inward, and binding with internal excess Cu^{2+} would prevent the formation of the catalytically active zinc-2,6-diacetylpyridine dioxime complex. Finally, a very interesting extension of this work involved the 38-Zn^{2+} -mediated catalysis of a liposome-encapsulated ester, which produced an amphiphilic carboxylic acid that made the lipid membrane sufficiently permeable to afford the triggered release of calcein from the vesicles.^[69c]

6. Vesicle Fusion and Adhesion

Another biomolecular process involving phospholipid membranes that has intrigued supramolecular chemists is the adhesion of membranes of different vesicles with or without subsequent membrane fusion. Aggregated vesicles with controlled adhesion may serve as cell-tissue mimics and fusion between cellular membranes is essential for basic biological process, for example, cell signaling, cell organization into tissues, or the entry of a virus into a cell.^[70] Despite the fact that membrane fusion is one of the most fundamental processes to life, understanding of this process is still limited.^[71] It is nonetheless believed that common steps, including recognition, docking, and fusion, are shared in cellular fusion mechanisms, regardless of

the cell type. Apart from the biological relevance, controlling the fusion process is of interest to supramolecular chemists and biochemists and could be applied in fields such as drug delivery and gene transfer. In this section, we review key works that have been conducted to expand knowledge of fusion of biomembranes with synthetic membrane-embedded amphiphiles. Although such synthetic amphiphiles differ from natural fusion systems, they constitute a simplified model and enable the study of biophysical determinant parameters involved in the fusion process. To induce vesicle adhesion and fusion, mainly two molecular recognition strategies been developed and studied, namely, metal-ion recognition and hydrogen bonding.

6.1. Vesicle adhesion

Sasaki and co-workers reported the first example of supramolecular vesicle adhesion mediated by metal-ion recognition almost 20 years ago.^[72] They noticed an increase in turbidity if Cu^{2+} ions were added to DSPC vesicles containing 5% pyrene-containing amphiphile **1** (see Figure 4) at lipid concentrations of around $100\ \mu\text{M}$; this is characteristic of vesicle aggregation (Figure 22). The resulting structure was characterized by means of electron microscopy, which showed columnar structured lipid bilayers with widths of 60 to 90 nm and lengths of 30 to 330 nm. Fluorescence measurements indicated that 2:1 (IDA/

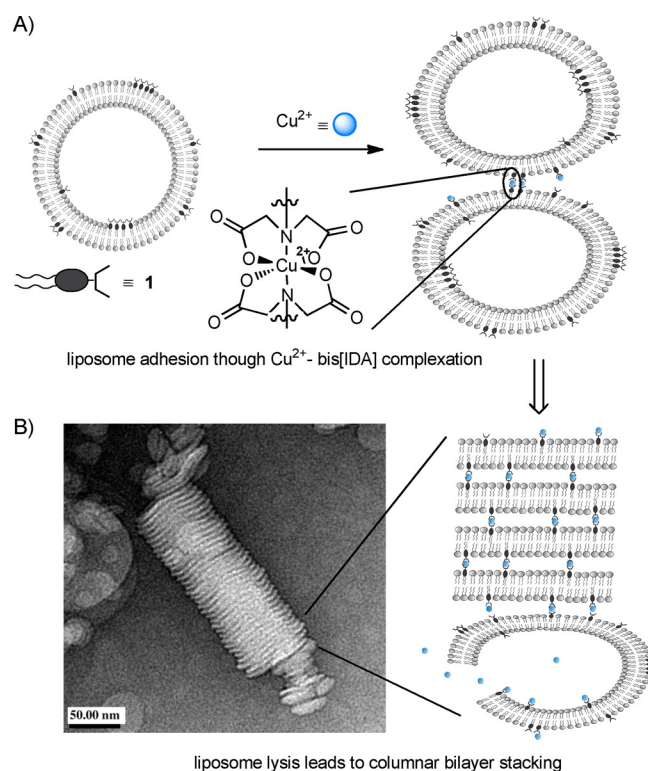


Figure 22. A) Proposed mechanism of lipid bilayer stack formation: the addition of Cu^{2+} leads to vesicle adhesion through Cu^{2+} -bis[IDA] complexation and causes membrane flattening. Subsequent lysis leads to bilayer stacks. H_2IDA : iminodiacetic acid. B) TEM image of columnar lipid bilayer stacks formed from 1/DSPC (5:95) liposomes after Cu^{2+} addition. Adapted with permission from ref. [72]. Copyright: 2001, American Chemical Society.

Cu^{2+}) intraliposome coordination did not occur. This is probably due to geometric restriction because the resulting IDA/ Cu^{2+} complex is oriented perpendicularly to the vesicle surface, which favors intervesicular binding with the IDA head group in a different vesicle. Further intervesicular binding of several molecules of **1** will lead to a flattening of the liposome surface, leading to liposome lysis and the formation of columnar stacks.

Webb and co-workers evaluated the effect of lateral phase separation (or lipid rafts) in vesicle adhesion by comparing cell-adhesion mimics without (**40**) and with a perfluoroalkyl segment (**41**) in their hydrophobic tails.^[73] Different from work by Sasaki and co-workers, they used the interaction of the $[\text{Cu}(\text{IDA})]^{2+}$ head group with the histidine amphiphile **42** for similar strengths to those of natural adhesive interactions ($\approx 10^3 \text{ M}^{-1}$).^[74] Due to the unfavorable interaction of the perfluoroalkyl groups with the hydrocarbon tails of the phospholipids, compound **41** was supposed to segregate into domains;^[75] this was confirmed by a much higher excimer-to-monomer (E/M) ratio in the emission spectrum of pyrene in a 1:1 mixture of DMPC/cholesterol vesicles (liquid-ordered phase) compared with that of DMPC vesicles in the liquid-crystalline phase. Compound **40**, lacking the perfluoroalkyl groups, served as a control and did not show any excimer emission, and thus, did not phase separate in vesicles (Figure 23).

If the DMPC/cholesterol vesicles containing 5 mol% perfluorinated **41** were mixed with DMPC/cholesterol vesicles containing **42**, a turbidity increase was observed, which implied significant vesicle aggregation, whereas control vesicles with **40** showed no indication of vesicle aggregation if they were mixed with vesicles containing **42**. This result suggests that domain formation in the membrane enhances intervesicular binding by bringing the multiple receptors into close spatial proximity, and thus, increasing the probability of forming multivalent interactions. To corroborate the importance of domain formation, vesicles with **41** composed of DMPC only were

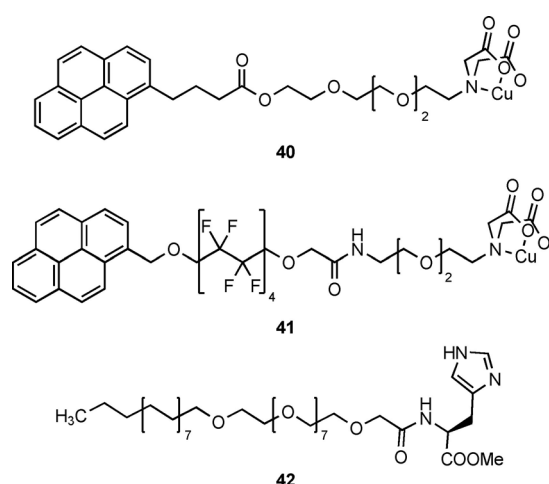


Figure 23. Cell-adhesion mimics **40–42**. Exploiting the interaction of the $[\text{Cu}(\text{IDA})]^{2+}$ head group with histidine gave aggregated vesicles. Aggregation was found to require domain formation of $[\text{Cu}(\text{IDA})]^{2+}$, and was most efficient for **41**, which contained a perfluorinated segment in the amphiphiles.

compared with DMPC/cholesterol vesicles. Also here, aggregate formation in the liquid-ordered phase of DMPC/cholesterol was more efficient than that in liquid-crystalline DMPC. A Job plot was in agreement with the 1:1 binding stoichiometry of the $[\text{Cu}(\text{IDA})]^{2+}$ head group with histidine and the results were also confirmed by means of fluorescence microscopy.

Paleos and Pantos also extensively explored vesicle adhesion and mainly used the interaction between phosphate- and guanidinium-containing amphiphiles embedded in complementary phospholipid vesicles.^[76] They often found that, after adhesion, multicompartimentalized vesicles resulted, which resembled eukaryotic cells with an outer membrane and several inner compartments.

6.2. Fusion by metal-ion recognition

One potential reason for the lack of controlled fusion in the Cu^{2+} -bis[IDA] system reported by Sasaki and co-workers (Figure 22) involves the formation of a pore connecting the two aqueous compartments of the vesicles, which is sufficiently large to allow the Cu^{2+} ions to enter into the inner compartment. Subsequent binding with the inner IDA head groups could then produce extra tension, which finally causes vesicle lysis. As a step beyond such relatively uncontrolled vesicle aggregation, different fusion systems were subsequently developed based on the binding of di- or trivalent metal cations to amphiphilic ligands. The amphiphilic ligands were designed to partition into the lipid membrane and form metal/ligand complexes. After the addition of metal cations, complexation brings two vesicles into close proximity to induce docking and finally fusion.

Lehn and co-workers equipped bipyridines with PEG chains of varying length and a terminal hexadecyl chain to afford amphiphiles **43–45**, which underwent vesicle-vesicle adhesion and fusion of LUVs upon addition of appropriate metal ions (Figure 24).^[77] The addition of Co^{2+} and Ni^{2+} led to intervesicular complex formation with the bipyridine head groups, and subsequent membrane fusion produced giant MLVs of several micrometers in diameter. Absorption spectroscopy indicated that complex formation proceeded within the first 30 min, whereas light scattering owing to vesicle fusion and concomitant size increase was only noted after much longer incubation times of 22 h.

Vesicle fusion without content leakage was unambiguously demonstrated by means of fluorescence microscopy with vesicles containing encapsulated sulforhodamine B. After the incubation of the LUVs with Ni^{2+} , strongly fluorescent giant vesicles were observed, whereas the absence of extravascular fluorescence indicated that there was no dye leakage, and thus, no membrane rupture; this suggested that the fusion mechanism took place through pore opening between two vesicles. Interestingly, a critical threshold concentration of the amphiphiles in the membrane and a sufficient length of PEG spacers was required to provide an optimal accessibility for the metal cations to the bipyridine binding sites, and thus, afford vesicle fusion.

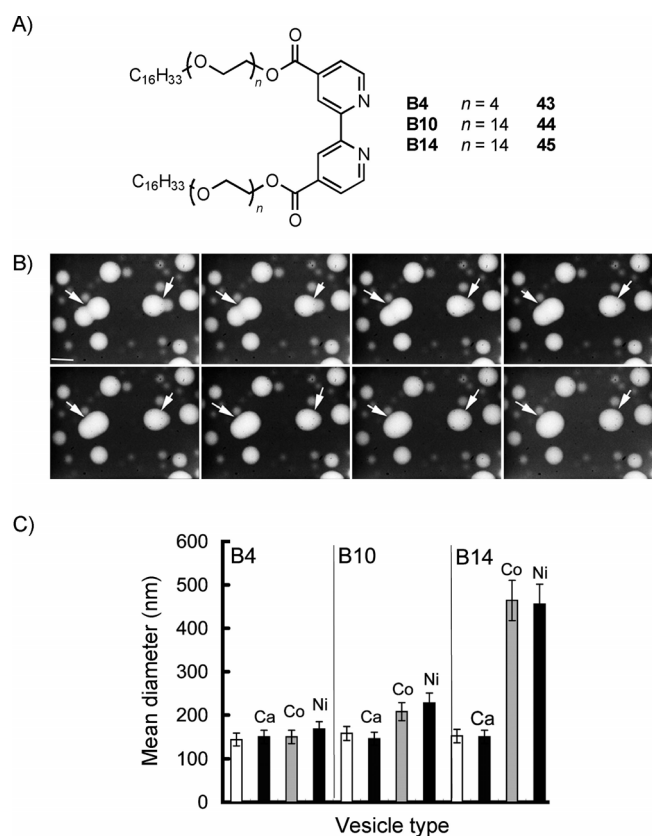


Figure 24. A) Structures of fusogenic amphiphiles **43–45**. B) Time evolution of vesicle fusion observed by means of fluorescence microscopy with sulforhodamine-loaded vesicles containing membrane-embedded B14. Images were recorded within 7 s (from upper left to lower right) after an incubation time of 12 h with Ni^{2+} ; scale bar: 10 μm . C) Mean diameters of vesicles with 3 mol% **43** (=B4), **44** (=B10), or **45** (=B14) in the absence of metal ions and after incubation with Ca^{2+} , Co^{2+} , or Ni^{2+} . Adapted with permission from ref. [77]. Copyright: 2004, National Academy of Sciences, USA.

In an extension of this work, β -diketone amphiphiles **46** (Figure 25) were inserted into GUVs, which acted as ligands for Eu^{3+} ions.^[78] To monitor fusion, two GUVs were isolated and brought into close proximity by using micropipettes, and after Eu^{3+} addition the process was monitored by using a fast digital camera. The authors investigated the effect of varying Eu^{3+} concentration on fusion and found that concentrations below 1 μM did not produce fusion, whereas Eu^{3+} concentrations above 1 mM caused vesicle lysis. Ni^{2+} ions were also investigated; these induced vesicle adhesion, but no fusion. If the ligand concentration was varied, a minimum concentration of 0.01 mol% was required for fusion, whereas no concentration dependence was noted above that threshold concentration.

It is noteworthy that, in the first example of this section, Sasaki and co-workers used DSPC,^[72] which has a higher T_m (55 °C) than that of the EYPC lipids used by Lehn and co-workers ($T_m = -5$ to -15 °C).^[77] Because DSPC lipids are in the gel state, and thus, more stable, this could be the reason for vesicle lysis, rather than fusion in the work by Sasaki et al., because diffusion and reorganization of the lipids of two adjacent vesicles would be slower in DSPC than that in EYPC.

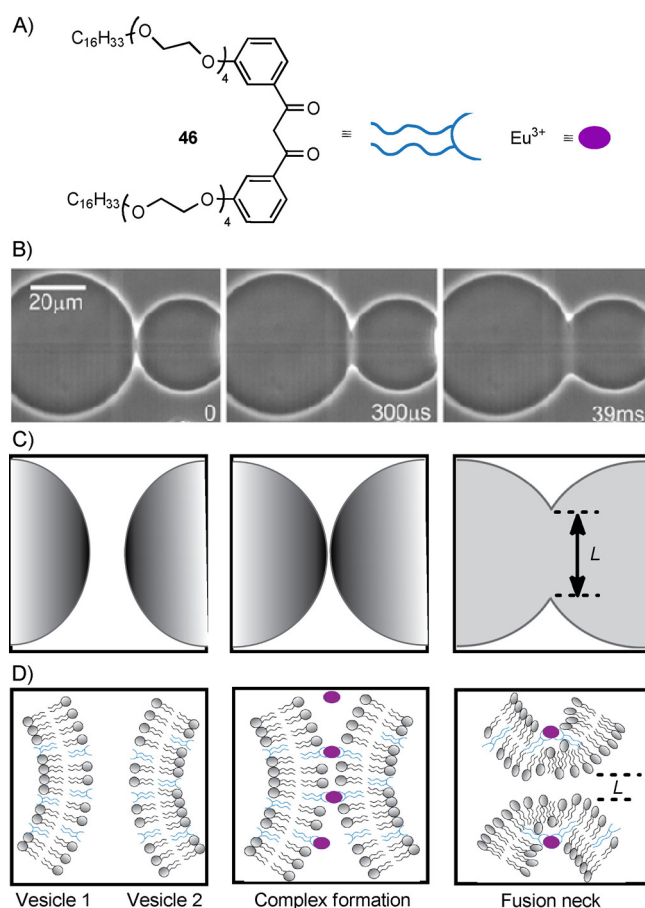


Figure 25. A) Chemical structure of β -diketone ligand **46**. B) Snapshots and C) micrometer scale schemes of the fusion of two functionalized vesicles. D) Proposed molecular rearrangements for ligand-mediated fusion. Adapted with permission from ref. [78]. Copyright: 2006, National Academy of Sciences, USA.

6.3. Fusion by hydrogen bonding

Hydrogen bonding has been explored as an alternative binding motif to induce vesicle adhesion and subsequent fusion.^[79] Notably, water is a highly competitive solvent, but hydrogen bonds at the water–membrane interface can be much stronger than those in water because of an altered microenvironment, including a reduced dielectric constant and a lower level of hydration at the interface.

To show the possibility of using hydrogen bonds in artificial fusion systems, Bong and co-workers used the well-established biological recognition motif of vancomycin with the dipeptide D-Ala-D-Ala (Figure 26).^[79a,b,80] The antimicrobial peptide magainin II^[81] was selected as a membrane anchor for vancomycin (**47**), due to its ability to insert into negatively charged membranes and thereby destabilize the membrane without causing fusion,^[82] and the D-Ala-D-Ala dipeptide was bound to the membrane as a POPE phospholipid derivative (**48**). If LUVs containing either membrane-anchored vancomycin or D-Ala-D-Ala were mixed, fusion proceeded, as shown by a rapid increase in light scattering, which reached, with time, a stable population with a larger size than that of the initial LUVs.^[79a] Fusion could be completely suppressed by the addition of unfunctionalized

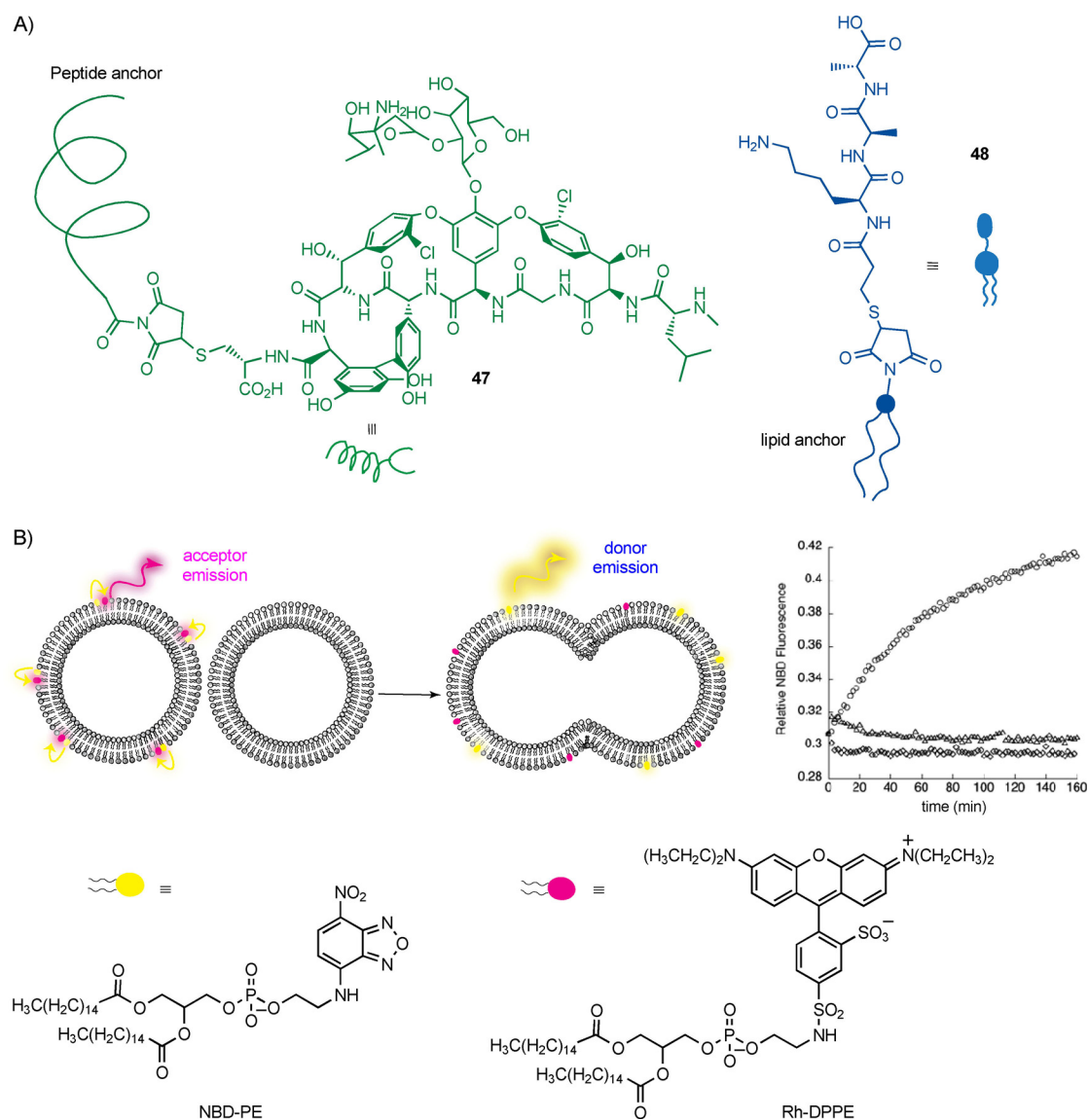


Figure 26. A) Artificial vesicle fusion by using the molecular recognition of D-Ala-D-Ala peptides by vancomycin, which were modified with the membrane anchors POPE and magainin II to afford **48** and **47**, respectively. B) Principle of the FRET dilution assay with the fluorescent lipids *N*-(7-nitrobenz-2-oxa-1,3-diazol-4-yl)amine (NBD)-PE (FRET donor) and *N*-(Lissamine rhodamine B sulfonyl)-1,2-dihexadecanoyl-*sn*-glycero-3-phosphoethanolamine (Rh-DPPE; FRET acceptor) and resulting fluorescence change of vesicles containing the FRET pair and **48** after the addition of vesicles containing i) **47** (circles, increase in NBD emission), ii) magainin II without vancomycin (diamonds, unchanged signal), or iii) **47** after blocking the **48**-containing vesicles with excess vancomycin (triangles, slight decrease). Adapted with permission from ref. [79a]. Copyright: 2006, American Chemical Society.

vancomycin, which saturated all binding sites at the D-Ala-D-Ala vesicles, thereby preventing the required intervesicular binding step. Notably, if vancomycin was coupled with a POPE phospholipid instead of magainin II, the resulting LUV mixture led to liposome aggregation without fusion; this demonstrated the necessity of a membrane-destabilizing agent to induce lipid mixing and subsequent fusion.

Membrane fusion was confirmed by using the established dilution assay (Figure 26B) based on the lipid-bound FRET pair NBD-PE and Rh-DPPE.^[83] Therefore, donor and acceptor lipids are incorporated within the same vesicles and mixed with unlabeled vesicles containing the complementary binding motif for fusion. Membrane fusion then causes fluorophore dilution in the membrane, leading to an increase of the average dis-

tance of the FRET pair, as signaled by an increase in donor fluorescence and a decrease in acceptor fluorescence (Figure 26B). As an additional control experiment, NBD at the outer membrane was reduced with sodium dithionite before fusion, which nonetheless showed the expected FRET signal change, and thus, indicated that fusion of inner and outer membranes and not only simple mixing of the outer lipid monolayer occurred.

It is interesting to note that the authors also investigated why fusion stopped after some time (Figure 27). During their investigations, they noted that a surface charge differential was required between the two liposome populations to afford efficient fusion.^[79a] It thus seemed likely that fusion stopped once the charge gradient had been eroded. Indeed, the addi-

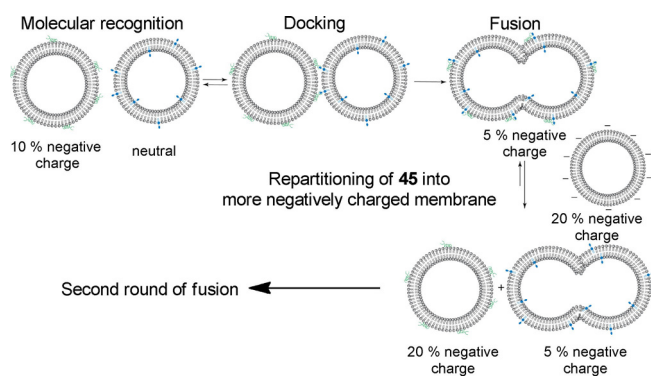


Figure 27. Catalytic, fusogenic activity of **45**. After fusion of vesicles with **45** containing 5% surface charge and vesicles with **46** containing no surface charge, further fusion stops because the surface charge difference has eroded, resulting in vesicles with 5% surface charge (upper row). Subsequent addition of vesicles with 20% surface charge restarts a second round of fusion by the repartitioning of **45** into the newly added vesicles. Adapted from ref. [79b]. Copyright: 2008, American Chemical Society.

tion of new vesicles containing 20% negatively charged POPG lipids, but no fusogen, gave a further change in FRET signal, in accordance with a further dilution of the membrane-bound FRET pair. Most likely, the positively charged fusogen **48** repartitions into the more negatively charged, freshly added, vesicle population with 20% POPG, which can subsequently fuse with the existing vesicles due to the re-established charge differential (20 vs. 5%). The fusogenic activity of **48** may thus be considered as catalytic because no further addition of fusogen is required to continue the fusion process, as long as the charge difference between the liposome populations to be fused is large enough.

To replace vancomycin and the dipeptide D-Ala-D-Ala, as biological recognition motifs of synthetic fusion systems,^[84] with a synthetic recognition motif, Bong and co-workers also explored the well-known^[85] hydrogen-bond-mediated interaction between cyanuric acid (CA) and melamine (ME).^[79d] Therefore, POPE lipids were functionalized with CA and ME to afford **49** and **50**, respectively (Figure 28). POPC vesicles containing **49** and **50** neither aggregated nor showed fusion, but replacement with DPPC vesicles indicated aggregation (at >20 mol% **49** and **50**) and slow membrane fusion (at >30 mol%), whereas vesicles containing only **49** and **50** showed efficient aggregation and fusion. This difference was attributed to a phase separation of **49** and **50** in DPPC, leading to a local concentration similar to that in pure vesicles, whereas the fluidity of the POPC membrane would lead to a much more diluted surface presentation of CA and ME.

With the goal of enhancing binding between the different vesicle populations, the trivalent POPE derivatives **51** and **52** were prepared. Because vesicles composed of **52** had a propensity for self-aggregation, experiments were performed with 5% **51** in EYPC membranes and 5% **52** in POPG/EYPC (20:80) membranes. If complementary vesicles were mixed, docking but no fusion was observed, whereas, if magainin II was added to the system, efficient vesicle fusion was observed; this indicated that destabilization by a disruptive membrane agent was required to afford fusion. To corroborate the hypothesis, the

POPE tail in **52** was replaced with a magainin II peptide tail and the resulting complementary vesicle mixtures indeed showed fusion. The authors also demonstrated fusion with supported lipid bilayers (SLBs) by adapting the solution-based FRET dilution assay. Vesicles with **52** and the FRET pair could be successfully fused to SLBs containing **51** and magainin II; this was indicated by dilution of the fluorescence into the SLBs and an accompanying fluorescence increase.

Finally, it is intriguing to note that Lehn and co-workers found that long PEG spacers were required for efficient fusion (Figures 24 and 25), whereas Bong and co-workers preferred relatively short linkers (Figures 26 and 28) to minimize the entropic cost of surface binding.^[77–79] This clearly shows that the determinants for artificial, supramolecular fusion systems are not yet understood and that the design of such systems still requires several rounds of optimization.

7. Summary and Outlook

Although nature has always inspired supramolecular chemists to mimic its ability to perform selective and highly regulated functions, it has proven a major challenge in recent decades to advance the field of supramolecular chemistry in that direction. Major milestones that have been addressed include enzyme mimics and supramolecular chemistry in water,^[3,86] but the sophistication level of even the simplest natural systems has yet to be reached by supramolecular chemists. This clearly calls for increasing the complexity of supramolecular systems and one way to bring complexity to the next level is through the compartmentalization of supramolecular systems in biomembranes. Research into supramolecular chemistry in the biomembrane is presently driven mainly from a functional point of view, with impressive examples of mimicking fundamental functions of live cells, such as membrane transport, vesicle fusion, and the role of lipid domain formation and reorganization in molecular recognition. However, major challenges still remain. For example, if simple 1:1 supramolecular binding affinities were compared in homogeneous solution and in the lipid bilayer membrane, about 1000-fold higher^[31a] and lower^[34] binding affinities were reported, and both effects have been explained by the microenvironment of the lipid bilayer. This illustrates that the factors that determine binding affinities at the interfacial region of hydrophobic structures still remain unknown.^[87] Physical-organic and supramolecular chemists, who have devised numerous strategies to determine binding affinities and map physicochemical parameters in microenvironments, are thus well trained to contribute to a deeper understanding of binding phenomena at interfaces. Notably, the possibility of significantly increasing the binding affinities or tailoring the selectivity of supramolecular systems by embedding them into biomembranes has, from a practical point of view, vast potential for the development of enhanced supramolecular sensor systems. Besides these fundamental, physicochemical aspects of supramolecular chemistry in biomembranes, functional studies, in particular, on membrane transport, have provided very valuable roadmaps for the future development of supramolecular functional systems in bio-

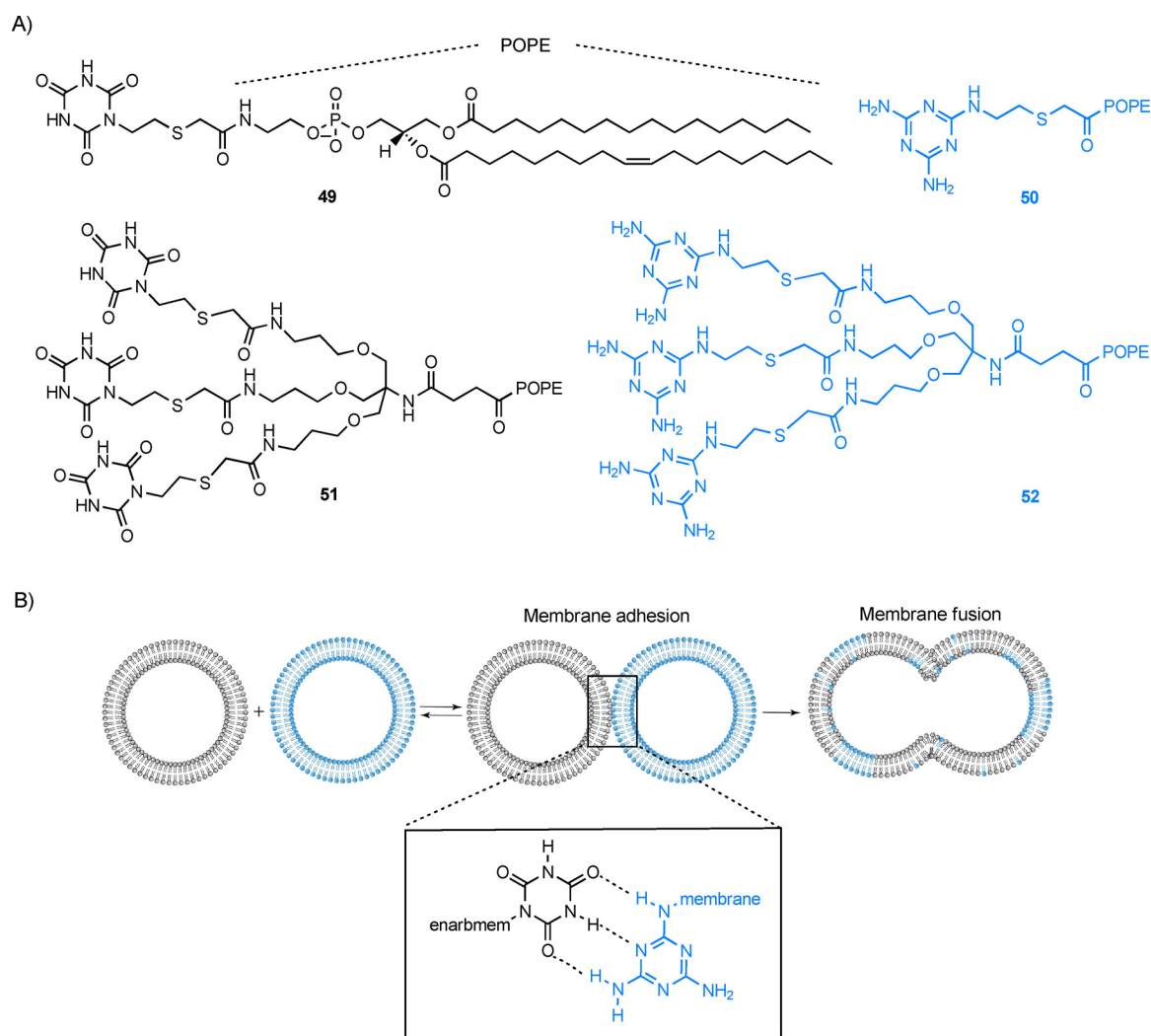


Figure 28. A) Chemical structures of a synthetic fusion system based on the interaction of ME with CA. B) Vesicle adhesion and fusion through hydrogen bonding between CA and ME derivatives.

membranes. Although supramolecular chemists rely largely on structural studies in homogeneous solution by using, for example, NMR spectroscopy, the concentrations of membrane-bound supramolecular functional systems are often too low and the spectra suffer from line broadening. As a consequence, other techniques, such as fluorescence or CD spectroscopy, have been applied to relate structure and supramolecular functions, most often involving carefully designed control experiments. It is also worth mentioning that structural studies are not always meaningful, for example, it has been noted by supramolecular chemists and researchers in the field of CPPs that the formation of the membrane-active structure is intrinsically dynamic and that only a subpopulation of the thermodynamic equilibrium is responsible for membrane transport.^[88] In addition, other challenges remain, for example, a versatile method to prepare artificial liposomes with an asymmetric distribution of molecules in the inner and outer leaflet would be desirable to study signal transduction systems.

Overall, supramolecular chemistry in the biomembrane presents an intellectual challenge for creative scientific thinking,

which can be demanding, but is, at the same time, also entertaining and satisfying. We believe that the time is ripe for exciting developments in the field of selective and stimuli-responsive membrane transport systems relying on supra-biomolecular recognition fueled by a better understanding of the biomembrane.

Acknowledgements

We are thankful for financial support from the DFG (HE 5967/4-1), from the Alexander-von-Humboldt Foundation (A.B.-B.), and from Jacobs University Bremen. Furthermore, we would like to thank Prof. Dr. Werner M. Nau for his generous and constant support, as well as for innumerable and valuable discussions.

Conflict of Interest

The authors declare no conflict of interest.

Keywords: liposomes • membranes • molecular devices • molecular recognition • receptors

- [1] S. J. Singer, G. L. Nicolson, *Science* **1972**, *175*, 720–731.
- [2] a) J. W. Steed, J. L. Atwood, *Supramolecular Chemistry*, 2nd ed., Wiley, Chichester, **2009**; b) J.-M. Lehn, *Angew. Chem. Int. Ed. Engl.* **1988**, *27*, 89–112; *Angew. Chem.* **1988**, *100*, 91–116.
- [3] R. Breslow, *Artificial Enzymes*, Wiley-VCH, Weinheim, **2005**.
- [4] C. J. Pedersen, *Angew. Chem. Int. Ed. Engl.* **1988**, *27*, 1021–1027; *Angew. Chem.* **1988**, *100*, 1053–1059.
- [5] a) S. H. Gellman, *Acc. Chem. Res.* **1998**, *31*, 173–180; b) D. Seebach, K. Namoto, Y. R. Mahajan, P. Bindschädler, R. Sustmann, M. Kirsch, N. S. Ryder, M. Weiss, M. Sauer, C. Roth, S. Werner, H.-D. Beer, C. Munding, P. Walde, M. Voser, *Chem. Biodiversity* **2004**, *1*, 65–97; c) S. Hecht, I. Huc, *Foldamers: Structure, Properties, and Applications*, Wiley-VCH, Weinheim, **2007**.
- [6] D. Marsh, *Biophys. J.* **2012**, *102*, 1079–1087.
- [7] a) D. Chandler, *Nature* **2005**, *437*, 640–647; b) P. S. Cremer, A. H. Flood, B. C. Gibb, D. L. Mobley, *Nat. Chem.* **2018**, *10*, 8–16; c) S. He, F. Biedermann, N. Vankova, L. Zhechkov, T. Heine, R. E. Hoffman, A. De Simone, T. T. Duignan, W. M. Nau, *Nat. Chem.* **2018**, *10*, 1252–1257.
- [8] a) S. Matile, A. Vargas Jentsch, J. Montenegro, A. Fin, *Chem. Soc. Rev.* **2011**, *40*, 2453–2474; b) X. Wu, E. N. W. Howe, P. A. Gale, *Acc. Chem. Res.* **2018**, *51*, 1870–1879; c) A. Fuertes, M. Juanes, J. R. Granja, J. Montenegro, *Chem. Commun.* **2017**, *53*, 7861–7871; d) Y.-M. Legrand, M. Barboiu, *Chem. Rec.* **2013**, *13*, 524–538; e) Y. Huo, H. Zeng, *Acc. Chem. Res.* **2016**, *49*, 922–930; f) W. Si, P. Xin, Z.-T. Li, J.-L. Hou, *Acc. Chem. Res.* **2015**, *48*, 1612–1619; g) I. Alfonso, R. Quesada, *Chem. Sci.* **2013**, *4*, 3009–3019; h) F. Otis, M. Auger, N. Voyer, *Acc. Chem. Res.* **2013**, *46*, 2934–2943; i) B. Gong, Z. Shao, *Acc. Chem. Res.* **2013**, *46*, 2856–2866; j) A. Vargas Jentsch, A. Hennig, J. Mareda, S. Matile, *Acc. Chem. Res.* **2013**, *46*, 2791–2800; k) F. De Riccardis, I. Izzo, D. Montesarchio, P. Tecilla, *Acc. Chem. Res.* **2013**, *46*, 2781–2790; l) J. K. W. Chui, T. M. Fyles, *Chem. Soc. Rev.* **2012**, *41*, 148–175; m) P. A. Gale, J. T. Davis, R. Quesada, *Chem. Soc. Rev.* **2017**, *46*, 2497–2519.
- [9] B. Alberts, A. Johnson, J. Lewis, D. Morgan, M. Raff, K. Roberts, P. Walter, *Molecular Biology of the Cell*, 6th ed., Garland Science, New York, **2014**.
- [10] a) T. Kunitake, *Angew. Chem. Int. Ed. Engl.* **1992**, *31*, 709–726; *Angew. Chem.* **1992**, *104*, 692–710; b) G. Yu, K. Jie, F. Huang, *Chem. Rev.* **2015**, *115*, 7240–7303.
- [11] J. N. Israelachvili, *Intermolecular and Surface Forces*, 3rd ed., Academic Press, San Diego, **2011**.
- [12] a) S. Uchiyama, K. Iwai, A. P. de Silva, *Angew. Chem. Int. Ed.* **2008**, *47*, 4667–4669; *Angew. Chem.* **2008**, *120*, 4745–4747; b) S. Uchiyama, E. Fukatsu, G. D. McClean, A. P. de Silva, *Angew. Chem. Int. Ed.* **2016**, *55*, 768–771; *Angew. Chem.* **2016**, *128*, 778–781.
- [13] a) J. F. Nagle, M. C. Wiener, *Biochim. Biophys. Acta Biomembranes* **1988**, *942*, 1–10; b) J. F. Nagle, S. Tristram-Nagle, *Biochim. Biophys. Acta, Biomembranes* **2000**, *1469*, 159–195; c) J. Sloniec, M. Schnurr, C. Witte, U. Resch-Genger, L. Schröder, A. Hennig, *Chem. Eur. J.* **2013**, *19*, 3110–3118; d) B. W. Koening, K. Gawrisch, *Biochim. Biophys. Acta, Biomembranes* **2005**, *1715*, 65–70.
- [14] a) J. Koralch, P. Schwillie, W. W. Webb, G. W. Feigenson, *Proc. Natl. Acad. Sci. USA* **1999**, *96*, 8461–8466; b) R. Meyer, A. F. P. Sonnen, W. M. Nau, *Langmuir* **2010**, *26*, 14723–14729.
- [15] a) J. F. Szoka, D. Papahadjopoulos, *Annu. Rev. Biophys. Bioeng.* **1980**, *9*, 467–508; b) D. D. Lasic, *Biochem. J.* **1988**, *256*, 1–11.
- [16] G. Gramlich, J. Zhang, M. Winterhalter, W. M. Nau, *Chem. Phys. Lipids* **2001**, *113*, 1–9.
- [17] N. Sakai, K. C. Brennan, L. A. Weiss, S. Matile, *J. Am. Chem. Soc.* **1997**, *119*, 8726–8727.
- [18] a) S. A. Wheaton, F. D. O. Ablan, B. L. Spaller, J. M. Trieu, P. F. Almeida, *J. Am. Chem. Soc.* **2013**, *135*, 16517–16525; b) H. Valkenier, N. López Mora, A. Kros, A. P. Davis, *Angew. Chem. Int. Ed.* **2015**, *54*, 2137–2141; *Angew. Chem.* **2015**, *127*, 2165–2169; c) A. Barba-Bon, Y.-C. Pan, F. Biedermann, D.-S. Guo, W. M. Nau, A. Hennig, *J. Am. Chem. Soc.* **2019**, *141*, 20137–20145.
- [19] P. Walde, K. Cosentino, H. Engel, P. Stano, *ChemBioChem* **2010**, *11*, 848–865.
- [20] a) B. Apellániz, J. L. Nieva, P. Schwillie, A. J. García-Sáez, *Biophys. J.* **2010**, *99*, 3619–3628; b) T. Shimanouchi, H. Umakoshi, R. Kuboi, *Langmuir* **2009**, *25*, 4835–4840.
- [21] A. Moscho, O. Orwar, D. T. Chiu, B. P. Modi, R. N. Zare, *Proc. Natl. Acad. Sci. USA* **1996**, *93*, 11443–11447.
- [22] A. P. de Silva, T. S. Moody, G. D. Wright, *Analyst* **2009**, *134*, 2385–2393.
- [23] a) B. T. Nguyen, E. V. Anslyn, *Coord. Chem. Rev.* **2006**, *250*, 3118–3127; b) A. Hennig, W. M. Nau in *Cucurbiturils and Related Macrocycles* (Ed.: K. Kim), Royal Society of Chemistry, Cambridge, **2020**, pp. 121–149.
- [24] a) A. Hennig, H. Bakirci, W. M. Nau, *Nat. Methods* **2007**, *4*, 629–632; b) R. N. Dsouza, A. Hennig, W. M. Nau, *Chem. Eur. J.* **2012**, *18*, 3444–3459; c) M. Schnurr, J. Sloniec-Myszk, J. Döpfert, L. Schröder, A. Hennig, *Angew. Chem. Int. Ed.* **2015**, *54*, 13444–13447; *Angew. Chem.* **2015**, *127*, 13645–13648; d) A. Hennig in *Supramolecular Systems in Biomedical Fields* (Ed.: H. J. Schneider), Royal Society of Chemistry, Cambridge, **2013**, pp. 355–396; e) Y.-C. Liu, S. Peng, L. Angelova, W. M. Nau, A. Hennig, *ChemistryOpen* **2019**, *8*, 1350–1354.
- [25] a) G. Ghale, A. G. Lanctôt, H. T. Kreissl, M. H. Jacob, H. Weingart, M. Winterhalter, W. M. Nau, *Angew. Chem. Int. Ed.* **2014**, *53*, 2762–2765; *Angew. Chem.* **2014**, *126*, 2801–2805; b) F. Biedermann, G. Ghale, A. Hennig, W. M. Nau, *ChemRxiv* **2019**, <https://dx.doi.org/10.26434/chemrxiv.9735152.v1>.
- [26] a) A. Stahl, A. I. Lazar, V. N. Muchemu, W. M. Nau, M. S. Ullrich, A. Hennig, *Anal. Bioanal. Chem.* **2017**, *409*, 6485–6494; b) M. Nilam, P. Gribbon, J. Reinshagen, K. Cordts, E. Schwedhelm, W. M. Nau, A. Hennig, *SLAS Discovery* **2017**, *22*, 906–914.
- [27] Y.-C. Liu, W. M. Nau, A. Hennig, *Chem. Commun.* **2019**, *55*, 14123–14126.
- [28] a) A. Hennig, A. Hoffmann, H. Borchering, T. Thiele, U. Schedler, U. Resch-Genger, *Chem. Commun.* **2011**, *47*, 7842–7844; b) A. Hennig, H. Borchering, C. Jaeger, S. Hatami, C. Würth, A. Hoffmann, K. Hoffmann, T. Thiele, U. Schedler, U. Resch-Genger, *J. Am. Chem. Soc.* **2012**, *134*, 8268–8276; c) S. Zhang, Z. Domínguez, K. I. Assaf, M. Nilam, T. Thiele, U. Pischel, U. Schedler, W. M. Nau, A. Hennig, *Chem. Sci.* **2018**, *9*, 8575–8581; d) M. Nilam, M. Ahmed, M. A. Alnajjar, A. Hennig, *Analyst* **2019**, *144*, 579–586.
- [29] a) D. Charych, J. Nagy, W. Spevak, M. Bednarski, *Science* **1993**, *261*, 585–588; b) S. Kolusheva, R. Zadnarm, T. Schrader, R. Jelinek, *J. Am. Chem. Soc.* **2006**, *128*, 13592–13598; c) D. J. Ahn, J.-M. Kim, *Acc. Chem. Res.* **2008**, *41*, 805–816; d) J. Wu, A. Zawistowski, M. Ehrmann, T. Yi, C. Schmuck, *J. Am. Chem. Soc.* **2011**, *133*, 9720–9723; e) O. Yarimaga, J. Jaworski, B. Yoon, J.-M. Kim, *Chem. Commun.* **2012**, *48*, 2469–2485; f) X. Chen, G. Zhou, X. Peng, J. Yoon, *Chem. Soc. Rev.* **2012**, *41*, 4610–4630; g) Q. Xu, S. Lee, Y. Cho, M. H. Kim, J. Bouffard, J. Yoon, *J. Am. Chem. Soc.* **2013**, *135*, 17751–17754.
- [30] a) K. Ariga, T. Kunitake, *Acc. Chem. Res.* **1998**, *31*, 371–378; b) O. Molt, D. Rübeling, T. Schrader, *J. Am. Chem. Soc.* **2003**, *125*, 12086–12087; c) R. Zadnarm, T. Schrader, *J. Am. Chem. Soc.* **2005**, *127*, 904–915.
- [31] a) D. R. Shnek, D. W. Pack, F. H. Arnold, D. Y. Sasaki, *Angew. Chem. Int. Ed. Engl.* **1995**, *34*, 905–907; *Angew. Chem.* **1995**, *107*, 994–996; b) D. Y. Sasaki, B. E. Padilla, *Chem. Commun.* **1998**, 1581–1582; c) D. Y. Sasaki, T. A. Waggoner, J. A. Last, T. M. Alam, *Langmuir* **2002**, *18*, 3714–3721; d) J. L. Pincus, C. Jin, W. Huang, H. K. Jacobs, A. S. Gopalan, Y. Song, J. A. Shelnut, D. Y. Sasaki, *J. Mater. Chem.* **2005**, *15*, 2938–2945; e) J. A. Last, T. A. Waggoner, D. Y. Sasaki, *Biophys. J.* **2001**, *81*, 2737–2742.
- [32] B. Gruber, S. Stadlbauer, K. Woinaroschy, B. König, *Org. Biomol. Chem.* **2010**, *8*, 3704–3714.
- [33] B. Gruber, S. Stadlbauer, A. Späth, S. Weiss, M. Kalinina, B. König, *Angew. Chem. Int. Ed.* **2010**, *49*, 7125–7128; *Angew. Chem.* **2010**, *122*, 7280–7284.
- [34] A. Hennig, S. Hatami, M. Spieles, U. Resch-Genger, *Photochem. Photobiol. Sci.* **2013**, *12*, 729–737.
- [35] A. Müller, B. König, *Chem. Commun.* **2014**, *50*, 12665–12668.
- [36] R. C. Major, X. Y. Zhu, *J. Am. Chem. Soc.* **2003**, *125*, 8454–8455.
- [37] E. L. Doyle, C. A. Hunter, H. C. Phillips, S. J. Webb, N. H. Williams, *J. Am. Chem. Soc.* **2003**, *125*, 4593–4599.
- [38] H. Jiang, B. D. Smith, *Chem. Commun.* **2006**, 1407–1409.
- [39] B. Gruber, S. Balk, S. Stadlbauer, B. König, *Angew. Chem. Int. Ed.* **2012**, *51*, 10060–10063; *Angew. Chem.* **2012**, *124*, 10207–10210.
- [40] S. Banerjee, B. König, *J. Am. Chem. Soc.* **2013**, *135*, 2967–2970.
- [41] S. Banerjee, M. Bhuyan, B. König, *Chem. Commun.* **2013**, *49*, 5681–5683.

- [42] a) M. K. Johansson, R. M. Cook, J. Xu, K. N. Raymond, *J. Am. Chem. Soc.* **2004**, *126*, 16451–16455; b) A. Hennig, D. Roth, T. Enderle, W. M. Nau, *ChemBioChem* **2006**, *7*, 733–737; c) H. Sahoo, A. Hennig, M. Florea, D. Roth, T. Enderle, W. M. Nau, *J. Am. Chem. Soc.* **2007**, *129*, 15927–15934; d) E. K. Kainmüller, E. P. Ollé, W. Bannwarth, *Chem. Commun.* **2005**, 5459–5461.
- [43] M. Bhuyan, B. Koenig, *Chem. Commun.* **2012**, *48*, 7489–7491.
- [44] G. W. Gokel, A. Mukhopadhyay, *Chem. Soc. Rev.* **2001**, *30*, 274–286.
- [45] M. M. Tedesco, B. Ghebremariam, N. Sakai, S. Matile, *Angew. Chem. Int. Ed.* **1999**, *38*, 540–543; *Angew. Chem.* **1999**, *111*, 523–526.
- [46] P. Talukdar, G. Bollot, J. Mareda, N. Sakai, S. Matile, *J. Am. Chem. Soc.* **2005**, *127*, 6528–6529.
- [47] a) N. Sakai, J. Mareda, S. Matile, *Acc. Chem. Res.* **2005**, *38*, 79–87; b) N. Sakai, J. Mareda, S. Matile, *Acc. Chem. Res.* **2008**, *41*, 1354–1365.
- [48] G. Das, P. Talukdar, S. Matile, *Science* **2002**, *298*, 1600–1602.
- [49] V. Gorteau, F. Perret, G. Bollot, J. Mareda, A. N. Lazar, A. W. Coleman, D.-H. Tran, N. Sakai, S. Matile, *J. Am. Chem. Soc.* **2004**, *126*, 13592–13593.
- [50] P. Talukdar, G. Bollot, J. Mareda, N. Sakai, S. Matile, *Chem. Eur. J.* **2005**, *11*, 6525–6532.
- [51] C. P. Wilson, S. J. Webb, *Chem. Commun.* **2008**, 4007–4009.
- [52] C. P. Wilson, C. Boglio, L. Ma, S. L. Cockroft, S. J. Webb, *Chem. Eur. J.* **2011**, *17*, 3465–3473.
- [53] U. Devi, J. R. D. Brown, A. Almond, S. J. Webb, *Langmuir* **2011**, *27*, 1448–1456.
- [54] C. J. E. Haynes, J. Zhu, C. Chimerel, S. Hernández-Ainsa, I. A. Riddell, T. K. Ronson, U. F. Keyser, J. R. Nitschke, *Angew. Chem. Int. Ed.* **2017**, *56*, 15388–15392; *Angew. Chem.* **2017**, *129*, 15590–15594.
- [55] X. Hu, N. Liu, H. Yang, F. Wu, X. Chen, C. Li, X. Chen, *Chem. Commun.* **2019**, *55*, 3008–3011.
- [56] T. Muraoka, T. Endo, K. V. Tabata, H. Noji, S. Nagatoishi, K. Tsumoto, R. Li, K. Kinbara, *J. Am. Chem. Soc.* **2014**, *136*, 15584–15595.
- [57] J. Gravel, J. Kempf, A. Schmitzer, *Chem. Eur. J.* **2015**, *21*, 18642–18648.
- [58] S. Peng, A. Barba-Bon, Y.-C. Pan, W. M. Nau, D.-S. Guo, A. Hennig, *Angew. Chem. Int. Ed.* **2017**, *56*, 15742–15745; *Angew. Chem.* **2017**, *129*, 15948–15951.
- [59] a) T. Miyatake, M. Nishihara, S. Matile, *J. Am. Chem. Soc.* **2006**, *128*, 12420–12421; b) A. Hennig, G. J. Gabriel, G. N. Tew, S. Matile, *J. Am. Chem. Soc.* **2008**, *130*, 10338–10344; c) S. M. Butterfield, T. Miyatake, S. Matile, *Angew. Chem. Int. Ed.* **2009**, *48*, 325–328; *Angew. Chem.* **2009**, *121*, 331–334; d) T. Takeuchi, V. Bagnacani, F. Sansone, S. Matile, *ChemBioChem* **2009**, *10*, 2793–2799; e) T. Takeuchi, S. Matile, *J. Am. Chem. Soc.* **2009**, *131*, 18048–18049; f) T. Takeuchi, J. Montenegro, A. Hennig, S. Matile, *Chem. Sci.* **2011**, *2*, 303–307.
- [60] P. Barton, C. A. Hunter, T. J. Potter, S. J. Webb, N. H. Williams, *Angew. Chem. Int. Ed.* **2002**, *41*, 3878–3881; *Angew. Chem.* **2002**, *114*, 4034–4037.
- [61] P. T. Corbett, J. Leclaire, L. Vial, K. R. West, J.-L. Wietor, J. K. M. Sanders, S. Otto, *Chem. Rev.* **2006**, *106*, 3652–3711.
- [62] a) S. M. K. Davidson, S. L. Regen, *Chem. Rev.* **1997**, *97*, 1269–1280; b) S. L. Regen, *Curr. Opin. Chem. Biol.* **2002**, *6*, 729–735; c) M. Mukai, S. L. Regen, *Bull. Chem. Soc. Jpn.* **2017**, *90*, 1083–1087.
- [63] S. Turkyilmaz, W.-H. Chen, H. Mitomo, S. L. Regen, *J. Am. Chem. Soc.* **2009**, *131*, 5068–5069.
- [64] C. Wang, Y. Yu, S. L. Regen, *Angew. Chem. Int. Ed.* **2017**, *56*, 1639–1642; *Angew. Chem.* **2017**, *129*, 1661–1664.
- [65] H. P. Dijkstra, J. J. Hutchinson, C. A. Hunter, H. Qin, S. Tomas, S. J. Webb, N. H. Williams, *Chem. Eur. J.* **2007**, *13*, 7215–7222.
- [66] T. Schrader, M. Maue, M. Ellermann, *J. Recept. Signal Transduction* **2006**, *26*, 473–485.
- [67] K. Bernitzki, M. Maue, T. Schrader, *Chem. Eur. J.* **2012**, *18*, 13412–13417.
- [68] K. Bernitzki, T. Schrader, *Angew. Chem. Int. Ed.* **2009**, *48*, 8001–8005; *Angew. Chem.* **2009**, *121*, 8145–8149.
- [69] a) M. J. Langton, F. Keymeulen, M. Ciaccia, N. H. Williams, C. A. Hunter, *Nat. Chem.* **2017**, *9*, 426–430; b) M. J. Langton, N. H. Williams, C. A. Hunter, *J. Am. Chem. Soc.* **2017**, *139*, 6461–6466; c) M. J. Langton, L. M. Scriven, N. H. Williams, C. A. Hunter, *J. Am. Chem. Soc.* **2017**, *139*, 15768–15773.
- [70] Y. Okada, *Exp. Cell Res.* **1962**, *26*, 98–107.
- [71] a) E. H. Chen, E. N. Olson, *Trends Cell Biol.* **2004**, *14*, 452–460; b) E. H. Chen, E. N. Olson, *Science* **2005**, *308*, 369.
- [72] T. A. Waggoner, J. A. Last, P. G. Kotula, D. Y. Sasaki, *J. Am. Chem. Soc.* **2001**, *123*, 496–497.
- [73] R. J. Mart, K. P. Liem, X. Wang, S. J. Webb, *J. Am. Chem. Soc.* **2006**, *128*, 14462–14463.
- [74] a) G. S. Jacob, C. Kirmaier, S. Z. Abbas, S. C. Howard, C. N. Steingger, J. K. Welply, P. Scudder, *Biochemistry* **1995**, *34*, 1210–1217; b) M. S. Kent, H. Yim, D. Y. Sasaki, S. Satija, Y.-S. Seo, J. Majewski, *Langmuir* **2005**, *21*, 6815–6824.
- [75] a) R. Elbert, T. Folda, H. Ringsdorf, *J. Am. Chem. Soc.* **1984**, *106*, 7687–7692; b) S. J. Webb, K. Greenaway, M. Bayati, L. Trembleau, *Org. Biomol. Chem.* **2006**, *4*, 2399–2407.
- [76] C. M. Paleos, A. Pantos, *Acc. Chem. Res.* **2014**, *47*, 1475–1482.
- [77] A. Richard, V. Marchi-Artzner, M.-N. Lalloz, M.-J. Brienne, F. Artzner, T. Gulik-Krzywicki, M.-A. Guedeau-Boudeville, J.-M. Lehn, *Proc. Natl. Acad. Sci. USA* **2004**, *101*, 15279–15284.
- [78] C. K. Haluska, K. A. Riske, V. Marchi-Artzner, J.-M. Lehn, R. Lipowsky, R. Dimova, *Proc. Natl. Acad. Sci. USA* **2006**, *103*, 15841–15846.
- [79] a) Y. Gong, Y. Luo, D. Bong, *J. Am. Chem. Soc.* **2006**, *128*, 14430–14431; b) Y. Gong, M. Ma, Y. Luo, D. Bong, *J. Am. Chem. Soc.* **2008**, *130*, 6196–6205; c) M. Ma, D. Bong, *Acc. Chem. Res.* **2013**, *46*, 2988–2997; d) M. Ma, Y. Gong, D. Bong, *J. Am. Chem. Soc.* **2009**, *131*, 16919–16926.
- [80] D. Kahne, C. Leimkuhler, W. Lu, C. Walsh, *Chem. Rev.* **2005**, *105*, 425–448.
- [81] M. Zasloff, *Proc. Natl. Acad. Sci. USA* **1987**, *84*, 5449.
- [82] H. W. Huang, *Biochim. Biophys. Acta Biomembr.* **2006**, *1758*, 1292–1302.
- [83] a) D. K. Struck, D. Hoekstra, R. E. Pagano, *Biochemistry* **1981**, *20*, 4093–4099; b) S. Matile, N. Sakai, A. Hennig in *Supramolecular Chemistry: From Molecules to Nanomaterials, Vol. 2: Techniques* (Eds.: P. A. Gale, J. W. Steed), Wiley, Hoboken, **2012**, pp. 473–500.
- [84] G. Stengel, R. Zahn, F. Höök, *J. Am. Chem. Soc.* **2007**, *129*, 9584–9585.
- [85] a) J. A. Zerkowski, C. T. Seto, G. M. Whitesides, *J. Am. Chem. Soc.* **1992**, *114*, 5473–5475; b) L. J. Prins, J. Huskens, F. de Jong, P. Timmerman, D. N. Reinhoudt, *Nature* **1999**, *398*, 498–502; c) L. J. Prins, F. De Jong, P. Timmerman, D. N. Reinhoudt, *Nature* **2000**, *408*, 181–184; d) L. J. Prins, D. N. Reinhoudt, P. Timmerman, *Angew. Chem. Int. Ed.* **2001**, *40*, 2382–2426; *Angew. Chem.* **2001**, *113*, 2446–2492.
- [86] a) G. V. Oshovsky, D. N. Reinhoudt, W. Verboom, *Angew. Chem. Int. Ed.* **2007**, *46*, 2366–2393; *Angew. Chem.* **2007**, *119*, 2418–2445; b) A. P. Davis, S. Kubik, A. Dalla Cort, *Org. Biomol. Chem.* **2015**, *13*, 2499–2500; c) S. Kubik, *Supramolecular Chemistry in Water*, Wiley-VCH, Weinheim, **2019**.
- [87] C. D. Ma, C. Wang, C. Acevedo-Vélez, S. H. Gellman, N. L. Abbott, *Nature* **2015**, *517*, 347–350.
- [88] a) Y. Baudry, G. Bollot, V. Gorteau, S. Litvinchuk, J. Mareda, M. Nishihara, D. Pasini, F. Perret, D. Ronan, N. Sakai, M. R. Shah, A. Som, N. Sordé, P. Talukdar, D.-H. Tran, S. Matile, *Adv. Funct. Mater.* **2006**, *16*, 169–179; b) M. Di Pisa, G. Chassaing, J.-M. Swiecicki, *Biochemistry* **2015**, *54*, 194–207.

Manuscript received: October 22, 2019

Accepted manuscript online: December 5, 2019

Version of record online: January 30, 2020